MicroRNA-27a mitigates hyperlipidemia and atherosclerosis by modulating cholesterol homeostasis

by

Abrar A. Khan[1], Heena Agarwal[2,a], S. Santosh Reddy[2,3,a], Vikas Arige[1,a], Vinayak Gupta[1], Ananthamohan Kalyani[1], G. Bhanuprakash Reddy[4], Madhu Dikshit[5], Manoj K. Barthwal[2], Nitish R. Mahapatra[1]

from the

[1]Department of Biotechnology, Bhupat and Jyoti Mehta School of Biosciences, Indian Institute of Technology Madras, Chennai 600036, India

[2]Pharmacology Division, CSIR-Central Drug Research Institute, Lucknow 226031, India

[3]Academy of Scientific and Innovative Research (AcSIR), New Delhi 110025, India

[4]Biochemistry Division, National Institute of Nutrition, Jamia Osmania PO, Hyderabad 500007, India

[5]Translational Health Science and Technology Institute, Faridabad 121001, India

[a] These authors contributed equally to this work.

Short title: Regulation of cholesterol homeostasis by miR-27a

Address for correspondence:

Dr. N. R. Mahapatra, Department of Biotechnology, Bhupat and Jyoti Mehta School of Biosciences, Indian Institute of Technology Madras, Chennai 600036, India. Tel: 91-44-2257-4128; E-mail: nmahapatra@iitm.ac.in

ABSTRACT

Hypercholesterolemia is a strong predictor of cardiovascular diseases that result in the largest number of mortality and morbidity worldwide. 3-Hydroxy-3-methylglutaryl-coenzyme A reductase gene (*Hmgcr*) coding for the rate-limiting enzyme in the cholesterol biosynthesis pathway is a crucial regulator of plasma cholesterol levels. However, the post-transcriptional regulation of Hmgcr remains poorly understood. Here, we show that *Hmgcr* is markedly inhibited, while miR-27a is highly induced in various cultured cell lines, human tissues as well as several rodent models of metabolic disorders (viz. genetically hypertensive blood pressure high mice, spontaneously hypertensive rats and high fat and high fructose diet-fed rats). Our *in vitro* data shows that miR-27a specifically interacts with the 3'-untranslated region of *Hmgcr* in murine and human hepatocytes. Our actinomycin D chase experiments demonstrate that miR-27a regulates Hmgcr by translational attenuation rather than mRNA degradation. Moreover, systematic *in silico* and functional analyses reveal that miR-27a expression is modulated by intracellular cholesterol level via Early Growth Response 1 transcription factor. Augmentation of miR-27a expression abrogates hyperlipidemia/atherosclerosis and improves cardiac function in high cholesterol diet-fed *Apoe*$^{-/-}$ mice. Pathway and gene expression analyses reveal that miR-27a also targets other genes (apart from *Hmgcr*) involved in cholesterol homeostasis. Our results suggest miR-27a as an attractive therapeutic candidate for clinical management of hypercholesterolemia and atherosclerosis.

SIGNIFICANCE STATEMENT

Elevated cholesterol level is an important risk factor for cardiovascular diseases. 3-hydroxy-3-methylglutaryl coenzyme A reductase (Hmgcr) is the rate-limiting enzyme in cholesterol biosynthesis pathway. Presently, statins (Hmgcr inhibitors) are used to lower the risk of cardiovascular complications by controlling the cholesterol level. However, statins show variable effects including serious adverse reactions in some patients. This work identifies microRNA-27a (miR-27a) as a crucial regulator of cholesterol biosynthesis as it targets many cholesterol regulatory genes including *Hmgcr*. We also

demonstrate the efficacy of miR-27a in improving cardiac function and alleviating atherosclerosis. Taken together, this study highlights the role of miR-27a in cholesterol regulation and provides a potential therapeutic candidate to treat elevated cholesterol level and atherosclerosis.

INTRODUCTION

Cardiovascular diseases (CVDs) remain the leading cause of global mortality and morbidity (1) despite extensive research over the past several decades. Among various determinants of CVDs, plasma concentration of cholesterol is an important factor as dyslipidemia (deregulated lipid and lipoprotein metabolism) may lead to multiple disease states including atherosclerosis, coronary artery disease, obesity, hypertension and type 2 diabetes (2-4). 3-hydroxy-3-methylglutaryl-coenzyme A (HMG-CoA) reductase gene (human: *HMGCR*, mouse/rat: *Hmgcr*) that codes for a ~ 97 kDa endoplasmic-reticulum membrane glycoprotein and catalyzes the rate-limiting step (HMG-CoA to mevalonate) in the cholesterol biosynthesis pathway (5-7) is, therefore, a critical modulator of dyslipidemia and consequent CVDs. Accordingly, statins which target HMG-CoA reductase are widely used to reduce high cholesterol levels and risk of CVDs (8, 9).

HMGCR gene is located on q arm of 5^{th} and 13^{th} chromosome in human and mouse, respectively. Several studies reported associations of SNPs in the *HMGCR* locus (viz. rs12654264, rs3846662, rs7703051, rs5908 rs12916, rs17238540 and rs3846663) with level of total cholesterol, LDL cholesterol and risk for dyslipidemia/stroke/blood pressure and coronary heart disease (10-17). The efficacy of statins is influenced by a haplotype consisting of three intronic single nucleotide polymorphisms (SNPs) (viz. rs17244841, rs3846662, and rs17238540) in *HMGCR* locus as this haplotype generates an alternatively spliced *HMGCR* transcript that is less sensitive to simvastatin/pravastatin inhibition (18-20). HMGCR expression/enzyme activity is modulated by feedback control mechanisms involving sterols and non-sterols (end-products of mevalonate metabolic pathway) at transcriptional and post-translational levels by family of sterol regulatory element binding proteins (SREBPs),

SREBP cleavage activated protein (SCAP), and insulin induced genes (Insig1 and Insig2) (7). However, the molecular mechanisms regulating *Hmgcr* expression at the post-transcriptional level are poorly understood.

MicroRNAs (miRNAs) are a class of small noncoding RNAs that control gene expression by translational repression and/or degradation (21). Dysregulation in the miRNA function may lead to various human diseases including cardiovascular and metabolic disorders (22-24). Indeed, recent studies have revealed that miRNAs play important roles in cardiovascular development, physiology, and pathophysiology (25-27). We undertook a systematic computational and extensive experimental analyses that revealed a crucial role for miR-27a in governing *Hmgcr* gene expression. In addition, this study, for the first time, provided evidence for post-transcriptional regulation of *Hmgcr* by miR-27a under basal and elevated cholesterol conditions. This study also highlights the previously unknown role of Egr1 in miR-27a expression. Interestingly, miR-27a targets multiple genes in addition to *Hmgcr* in the cholesterol biosynthesis/uptake pathways. In line with these *in vitro* findings, miRNA-27a shows efficient abrogation of hyperlipidemia and atherosclerosis in a well-established atherogenic disease model (*Apoe* $^{-/-}$ mice).

RESULTS

Comparative genomics analysis of mouse and rat *Hmgcr* gene sequences.

Although various resources are available for genetic mapping in mice and mouse models are highly useful to dissect the genetic basis of complex human diseases (28), most of the quantitative trait loci (QTL) studies have been performed in rats because measurement of cardiovascular phenotypes in mice is technically challenging. We mined the elevated lipid or cholesterol QTLs on *Hmgcr*-harboring chromosome 2 within the range of 26000000-28000000 bp from the Rat Genome Database (RGD) and detected six lipid-related QTLs (Fig.1A). The elevated lipid/cholesterol-QTLs and respective LOD [logarithm (base 10) of odds] scores retrieved from RGD are shown in Table 2. Interestingly, the QTL Stl27 (23837491-149614623 bp) that harbors *Hmgcr* gene (27480226-27500654 bp, RGD ID: 2803) displayed the highest linkage (LOD score=4.4) with blood triglyceride levels (Fig.1A). In addition, QTLs Stl32 (22612952-

67612952 bp) and Scl55 (26186097-142053534 bp) also harboring the *Hmgcr* locus displayed significant linkage with blood triglyceride levels (LOD score=3.2) and blood cholesterol levels (LOD score=2.83), respectively. Moreover, alignment of the mouse and rat genomic regions at *Hmgcr* locus using mVISTA showed >75% homology between these rodents at exons, introns and untranslated regions (Fig.1B). Interestingly, the extent of homology between each of the twenty *Hmgcr* exons in mouse and rat were, in general, higher (>85%) than the noncoding regions (Fig.1B). Thus, mouse *Hmgcr* appeared as a logical candidate gene for studying the mechanisms of hypercholesterolemia.

Identification of potential miRNAs involved in regulation of *Hmgcr*.

First, to identify the putative miRNA binding sites in the 3'-UTR of *Hmgcr* we performed an *in silico* analysis by using multiple bioinformatic algorithms (29). Only those miRNAs that were predicted by at least five algorithms were selected for further screening. Further, to shortlist the potentially functional miRNAs, those predicted miRNAs were base-paired with *Hmgcr* 3'-UTR to calculate the differences in hybridization free energy indicating the stability of the microRNA-mRNA interaction by two online tools namely PITA and RNAhybrid (*SI Appendix*, Table S2). In each case, the minimum number of nucleotides in seed sequence was selected as 6 and no mismatch or G:U wobble base-pairing was allowed in the region of seed sequence. The lower or more negative ΔG (<-10) or $\Delta\Delta G$ (<-20) value predicted by PITA/RNAhybrid represent stronger binding of the miRNA to the UTR. On following these selection procedures, 7 miRNAs (miR-27a, miR-27b, miR-708, miR-28, miR-351, miR-124 and miR-345) were shortlisted (Table 1). However, only miR-27a and miR-27b were further selected for our studies based on their reported roles in lipid metabolism (30).

Next, we probed for Hmgcr and miR-27a/b expression in three rodent models of metabolic syndrome viz. genetically hypertensive blood pressure high (BPH) *vs*. genetically hypotensive blood pressure low (BPL) mice, Spontaneously Hypertensive Rats (SHR) *vs*. Wistar Kyoto (WKY) rats and rats fed with high fructose and fat diet (HFHF) *vs*. rats on a normal chow diet regimen. Interestingly, Hmgcr protein expression was ~2-fold ($p<0.05$, *SI Appendix*, Fig.S1A) lower in BPH liver tissues than BPL. qPCR

analysis in the liver tissues of these models revealed differential expression of miR-27a and miR-27b in BPH and BPL mice. Specifically, the expression of miR-27a was found ~1.45- fold ($p<0.05$, *SI Appendix*, Fig.S1A) elevated in BPH tissue than BPL. On the other hand, the expression of miR-27b was ~3-fold ($p<0.05$) higher in BPL liver than BPH (*SI Appendix*, Fig.S2A). Likewise, Hmgcr and miR-27a/b levels were also analyzed in liver tissues of hypertensive rat models viz. SHR and WKY. Consistently, the Hmgcr protein expression was ~1.6-fold diminished in SHR liver tissues than WKY. Interestingly, miR-27a expression was ~2.5-fold higher in SHR than its normotensive counterpart, WKY ($p<0.05$, *SI Appendix*, Fig.S1B). There was no significant change in the miR-27b levels in SHR and WKY liver tissues (*SI Appendix*, Fig.S2B). In corroboration, the miR-27a levels were augmented by ~4.6-fold ($p<0.05$, *SI Appendix*, Fig.S1C) in normal chow-fed rats than high fat and fructose (HFHF)-fed rats while the Hmgcr levels were ~1.7-fold ($p<0.05$, *SI Appendix*, Fig.S1C) diminished in normal chow-fed rats. Taken together, only miR-27a showed an inverse correlation with *Hmgcr* expression in liver tissues of the aforementioned models indicating it as a promising candidate for functional characterization. Indeed, Watson-Crick base pairing between miR-27a and *Hmgcr* 3'-UTR (generated by miRanda) revealed that the 2-7 base seed sequence of miR-27a has perfect complementarity to its putative binding site present in the mouse *Hmgcr* 3'-UTR (Fig.2A)**.** Consistently, the expression of miR-27a and *Hmgcr* transcripts showed a significant negative correlation in mouse hepatocyte/neuroblast cells as well as rat liver/kidney/skeletal muscle tissues (Pearson r = -0.9550, $p<0.05$; Fig.2B).

Since the miR-27a binding site is highly conserved across mammals including humans (Fig.2C), we mined the hsa-miR-27a/b expression and *HMGCR* expression in different human tissues using miRmine, DASHR databases and GTEx portal. Interestingly, *HMGCR* expression was induced while miR-27a expression was inhibited in these tissues with a significant negative correlation (Fig.2D) in both miRmine (Pearson r = -0.9007, $p<0.05$) and DASHR miRNA expression databases (Pearson r = -0.8830, $p<0.05$). On the other hand, miR-27b expression did not show any such inverse correlation with *HMGCR* expression in the same tissues (*SI Appendix*, Fig.S2D).

Direct interaction of miR-27a with *Hmgcr* 3'-UTR down-regulates Hmgcr protein level in mouse and human hepatocytes.

To examine whether miR-27a directly interacts with *Hmgcr*, pre-miRNA plasmid expressing miR-27a, was co-transfected with the m*Hmgcr* 3'UTR/luciferase construct into mouse and human hepatocytes (AML12 and HuH-7 cells, respectively; Fig.3A, B). Indeed, over-expression of miR-27a caused a dose-dependent reduction in the m*Hmgcr* 3'UTR reporter activity in both AML12 (one-way ANOVA $F=10.95$, up to ~85%, $p<0.0001$) and HuH-7 cells (one-way ANOVA $F=7.31$, up to ~34%, $p<0.001$). In contrast, co-transfection of the m*Hmgcr* 27a mut 3'UTR construct (devoid of the miR-27a binding site) with the miR-27a expression plasmid showed no significant reduction in the 3'UTR reporter activity (Fig.3A, B). Further, qPCR analysis showed that over-expression of pre-miR-27a led to a dose-dependent increase in the expression of the mature form of miR-27a in AML12 (one-way ANOVA $F=10.48$, up to ~1770%, $p<0.01$) and HuH-7 (one-way ANOVA $F=4.66$, up to ~125%, $p<0.05$) cells; consistently, endogenous HMGCR protein level was also diminished (Fig.3C and D).

Despite the predicted binding site of miR-27b in the *Hmgcr* 3'-UTR, co-transfection of different concentrations of miR-27b expression plasmid did not cause significant decrease in m*Hmgcr* 3'UTR reporter activity (*SI Appendix*, Fig.S3A). Moreover, to test the specificity of interactions of miR-27a with *Hmgcr* 3'-UTR, we carried out co-transfection experiments with miR-764 which does not have binding sites in the *Hmgcr* 3'-UTR region*;* no change in the *Hmgcr* 3'-UTR luciferase/reporter activity was observed (*SI Appendix*, Fig.S3B). Furthermore, transfection of locked nucleic acid inhibitor of 27a (LNA 27a) in AML12 cells led to enhancement of Hmgcr mRNA (by ~3.8-fold, $p<0.05$) and protein levels (Fig.4B, C). In line with these observations, AML12 cells transfected with miR-27a mimics showed diminished Hmgcr mRNA and protein levels (Fig.4E, F). In corroboration, RIP (ribonucleoprotein immunoprecipitation) assays with antibody against Ago2 (an integral component of RNA induced-Silencing Complex, RISC) showed enrichment of *HMGCR* (by ~5-fold, $p<0.01$) in the Ago2-immunoprecipitated RNA fraction of HuH-7 cells over-expressing miR-27a, thereby confirming the *in vivo* interaction of miR-27a with the *Hmgcr* 3'-UTR in the context of RISC (Fig.4G).

Role of intracellular cholesterol levels in miR-27a-mediated regulation of Hmgcr.

Because Hmgcr protein level is dependent on intracellular cholesterol level and regulated by a negative feed-back mechanism, we sought to determine whether modulation in endogenous cholesterol level affects the post-transcriptional regulation of *Hmgcr* (31). Accordingly, AML12 cells were treated with different concentrations of either cholesterol (5, 10 and 20 µg/ml) or methyl-β-cyclodextrin (MCD, a well-known cyclic oligosaccharide that reduces intracellular cholesterol levels; 1, 2.5 and 5 mM) followed by Western blot analysis for Hmgcr (Fig.5A, B). Since 20 µg/ml of cholesterol or 5 mM of MCD showed effective reduction or augmentation in Hmgcr protein level, respectively, these doses were used for further experiments. Indeed, cholesterol treatment showed ~1.9-fold ($p<0.05$) enhancement of miR-27a levels (Fig.5C). In concordance, cholesterol depletion by MCD caused a ~3-fold ($p<0.05$) reduction in the endogenous expression of miR-27a (Fig.5D). Increase/decrease in the intracellular cholesterol level was confirmed by Filipin staining (Fig.5E, F). Further, ribonucleoprotein immunoprecipitation assays using anti-Ago2 antibody in cholesterol-treated HuH-7 cells revealed significant enrichment of *HMGCR* (~2.2-fold, $p<0.01$) (Fig.5G) and miR-27a levels (~1.7-fold, $p<0.001$) (Fig.5H) suggesting *in vivo* interaction of *HMGCR* with miR-27a under elevated cholesterol conditions. As a control, RNA fraction immunoprecipitated using pre-immune anti-mouse IgG antibody showed no significant difference in *HMGCR* levels between miR-27a over-expression and basal conditions (*SI Appendix*, Fig.S4).

Role of Egr1 in miR-27a expression under basal and modulated intracellular cholesterol conditions.

To understand the possible mechanism of regulation of miR-27a we predicted the putative transcription factor binding sites on the proximal miR-27a promoter domain (~500 bp) using two independent programs: LASAGNA and JASPAR (*SI Appendix*, Table S2). Egr (early growth response) 1, a zinc finger transcription factor predominantly expressed in the liver, plays a crucial role in the transcriptional regulation of most cholesterol biosynthesis genes including *Hmgcr* (32). These programs revealed

six Egr1 binding sites as two separate clusters in the selected region of miR-27a promoter domain (Fig.6A).

Next, we validated the role of Egr1 in the regulation of miR-27a expression by carrying out a series of co-transfection experiments. Over-expression of Egr1 caused a ~3-fold enhancement of miR-27a promoter activity (one-way ANOVA $F=36.41$, $p<0.0001$) (Fig.6B). In contrast, co-transfection of Egr1 shRNA expression plasmid with the miR-27a promoter construct resulted in a ~2.2-fold reduction in the miR-27a promoter activity (one-way ANOVA $F=6.955$, $p<0.05$; Fig.6C). A concomitant increase (~4-fold, $p<0.05$)/decrease (~2-fold, $p<0.05$) in the endogenous miR-27a levels upon Egr1 over-expression/down-regulation was also observed (Fig.6D, E). Thus, Egr1 may play a crucial role in the transcriptional activation of miR-27a. Indeed, chromatin immunoprecipitation (ChIP) assays confirm the *in vivo* interaction of Egr1 with the proximal (~-500 bp) promoter domain of the miR-27a in the context of chromatin. qPCR analysis using Egr1 antibody-immunoprecipitated chromatin revealed ~2.5-fold enrichment of the miR-27a promoter domain when P2 primer pair (mentioned in the *SI Appendix, SI Materials and Methods*) was used (Student's *t*-test, ~2.5-fold, $p<0.001$) (Fig.6F). No significant difference in the fold-enrichment over IgG was observed using Egr1 antibody immunoprecipitated chromatin for primer pair P1 (*SI Appendix*, Fig.S5) suggesting that the Egr1 sites predicted in this domain (Egr1 cluster 1) are non-functional. As Egr1 activates miR-27a promoter and cholesterol modulates miR-27a expression, we sought to test the effect of intracellular cholesterol on Egr1 expression. Indeed, Western blot analysis revealed that exogenous cholesterol treatment caused Egr1 augmentation (Fig.6G) while cholesterol depletion resulted in diminished Egr1 levels (Fig.6H) suggesting that intracellular cholesterol level regulates miR-27a expression via Egr1.

Regression of atherosclerosis and improvement of cardiac functions in *Apoe*$^{-/-}$ mice by miR-27a mimic

To test if miR-27a mimics can regress or mitigate the progression of diet-induced atherosclerosis, *Apoe*$^{-/-}$ mice on a high cholesterol diet regimen for 10 weeks were

injected with either saline or 5 mg/kg dose of miR-27a mimic or control oligo as lipid emulsion formulations (Fig.7A). Tissue analysis of miR-27a levels revealed ~4-fold ($p<0.05$), ~5.8-fold ($p<0.05$) and ~4.3-fold ($p<0.05$) up-regulation of miR-27a expression in the liver, heart and adipose tissues, respectively, in animals injected with miR-27a mimics. However, miR-27a levels remained unchanged in the kidney and brain of mice injected with miR-27a mimic as compared to the control oligo-injected group (Fig.7B). No significant differences were observed for various metabolic parameters between control oligo and saline-injected animals indicating that the control oligo has no effect on these parameters; hence, all further comparisons were made between miR-27a mimic and control oligo-injected mice (*SI Appendix*, Fig.S6).

Western blot analysis in liver tissues of these mice revealed diminished Hmgcr protein levels in miR-27a mimic-injected mice as compared to the control (Fig.7C). It is interesting to note that the anti-Hmgcr antibody detected a ~120 kDa band suggesting predominantly glycosylated form of the protein in these tissues. The hepatic cholesterol level in miR-27a-injected animals showed a modest decrease, which did not differ significantly in comparison to the control oligo-treated animals (Fig.7D).

Next, we assessed the effect of miR-27a mimics on the circulating lipid and glucose levels. These parameters were measured 4 days after the second injection of either the miR-27a mimic or control oligo. Interestingly, the miR-27a mimic-injected *Apoe*$^{-/-}$ mice showed reduced plasma total cholesterol (~1.5-fold, $p<0.001$), LDL cholesterol levels (~1.4-fold, $p<0.001$) and triglycerides (~1.3-fold, $p<0.01$) (Fig.7E, F and G). On the other hand, miR-27a mimic enhanced the plasma HDL cholesterol levels (~1.5-fold, $p<0.05$) (Fig.7H). The fasting blood glucose levels of the control oligo/miR-27a mimic-injected animals did not differ (*SI Appendix*, Fig.S7A). The body weight of the animals also remained unchanged after the miR-27a or control oligo injection (*SI Appendix*, Fig.S7B).

It is important to note that the decreases in plasma cholesterol were not accompanied by elevations in the plasma ALT, AST and CK levels indicating no obvious liver or muscle injury from the miR-27a mimic injections (Fig.7I, J and K). These findings suggest the therapeutic potential of miR-27a mimic as a safe and efficient cholesterol lowering agent.

We also examined the cardiac functions in these animals by echocardiography (Fig.8A). Interestingly, miR-27a-injected mice showed significant enhancements in LV internal diameters (LVIDd by ~1.16-fold, $p<0.05$ and LVIDs by ~1.3-fold, $p<0.05$; Fig.8B) and diminished LV posterior wall thickness (LVPWd by ~1.42-fold, $p<0.05$ and LVPWs by ~1.5-fold, $p<0.05$; Fig.8B) as compared to the control group. However, no change in the ejection fraction was observed between the two groups (data not shown). Furthermore, we visualized atherosclerotic plaques in the aortic arches and observed fewer plaques in the miR-27a mimic group compared to the control oligo group (Fig.8C). The vessel wall thickness at lesser curvature of the aortic arch measured by ultrasound imaging showed a significant reduction in arterial thickening in the miR-27a group (by ~2-fold, $p<0.05$; Fig.8D, E) as compared to the control oligo group. H&E staining of liver tissues from miR-27a-treated mice showed a marked decrease in lipid infiltration as compared to control oligo group (Fig.8F). Additionally, miR-27a-injected mice displayed diminished (by ~2.6-fold, $p<0.05$) lipid accumulation in the liver upon Oil red O staining (Fig.8F, G). The miR-27a-injected mice also showed a significant reduction of liver fibrosis as compared to the oligo control group (Fig.8H). Moreover, the control oligo-treated mice showed a predominant deposition of thick collagen type I fibers in comparison with miR-27a-treated mice as interpreted under polarized light microscopy of PSR (Picro Sirius Red)-stained liver sections (Fig.8H). Quantitative analysis of liver fibrosis indicated a ~2-fold ($p<0.05$) decrease in the percentage fibrotic area in miR-27a-injected animals as compared to the control oligo group (Fig.8I).

miR-27a represses Hmgcr by post-translational inhibition.

miRNAs act on their mRNA targets either by triggering mRNA degradation or translational repression. In order to unfold the mechanism of action of miR-27a on *Hmgcr*, mRNA stability assays using actinomycin D were carried out in AML12 cells over-expressing miR-27a (Fig.9). Hmgcr mRNA at different time points following incubation with actinomycin D were analyzed by qPCR in AML12 over-expressing miR-27a or control (without miR-27a transfection). Interestingly, no significant change in the Hmgcr mRNA half-life was observed on ectopic over-expression of miR-27a (Fig.9A, B).

However, the Hmgcr protein levels showed a time-dependent reduction following actinomycin D treatment in AML12 cells transfected with miR-27a (Fig.9C). In corroboration, over-expression of miR-27a in AML12 cells also did not alter the steady state Hmgcr mRNA levels (*SI Appendix*, Fig.S8). Thus, the repression of Hmgcr by miR-27a is mediated via translational attenuation rather than mRNA degradation.

miR-27a down-regulates multiple genes in the cholesterol regulatory pathways.

In line with our observations and reported role of miR-27a in lipid metabolism, we tested if miR-27a targets other genes crucial for cholesterol homeostasis. Interestingly, TargetScan, miRWalk and RNAhybrid predictions coupled with PANTHER pathway analysis revealed six additional cholesterol biosynthesis-related gene targets: 3-Hydroxy-3-Methylglutaryl-CoA synthase 1 (*Hmgcs1*), Mevalonate kinase (*Mvk*), Diphosphomevalonate decarboxylase (*Mvd*), Geranylgeranyl pyrophosphate synthase (*Ggps1*), Squalene synthase (*Fdft1*), Squalene epoxidase (*Sqle*) indicating that miR-27a might regulate multiple genes in the cholesterol biosynthesis pathway (Fig.10 A). Indeed, miR-27a mimic treatment in AML12 cells or *Apoe*$^{-/-}$ mice diminished the expression of *Mvk*, *Fdft1*, *Sqle*, *Ggps1* and *Mvd* (Fig.10B, C). In addition, miR-27a augmentation also resulted in diminished expression of crucial genes responsible for lipoprotein uptake viz. low density lipoprotein receptor (*Ldlr*) and Scavenger Receptor Class B Member1 (*Scarb1*) (*SI Appendix*, Fig.S9). Thus, miR-27a seems to play a key role in the global regulation of genes involved cholesterol homeostasis.

DISCUSSION

Overview

Although statins are widely used for the treatment of hypercholesterolemia and to lower the risk of cardiovascular complications, these drugs exhibit altered efficacies and adverse effects including myalgias, muscle or gastrointestinal cramps and other symptoms (33). These safety and efficacy concerns over the long-term use of statins call for alternative therapeutic interventions for lowering plasma lipids. The emerging

role of miRNAs as crucial regulators of lipid metabolism has been documented (34). As such, they serve as promising candidates for miRNA-based therapeutics. Moreover, owing to their short sequence and conservation across most vertebrates, miRNAs are easy therapeutic targets and the same miRNA-modulating compound can be used both for the pre-clinical studies and in clinical trials (35). The role of miRNAs in regulation of *Hmgcr*, however, is only partially understood. In this study, we undertook a systematic approach to identify the key miRNAs that may regulate *Hmgcr* gene expression under basal as well as pathophysiological conditions. Our extensive computational analysis using multiple bioinformatic algorithms coupled with experimental analysis (miR-27a over-expression/downregulation experiments along with Ago2-ribonucleoprotein immunoprecipitation assays) identified miR-27a as a key regulator of *Hmgcr* expression (Figs.3 and 4). Of note, these findings are in concordance with a previous study reporting the repression of *HMGCR* 3'-UTR luciferase activity in HuH-7 cells transfected with miR-27 mimics (36). We also tested the effect of miR-27a mimic on the plasma lipid level, atherosclerosis and cardiac functions in a high cholesterol diet-fed atherosclerotic mouse model (Figs.7 and 8).

Regulation of Hmgcr expression by miR-27a is conserved across various mammalian species.

Alignment of *Hmgcr*-3'UTR sequence of various mammalian species harboring the miR-27a binding site (human, rat, hedgehog, rabbit, chimpanzee, cow, rhesus, shrew, dog, cat, armadilo, elephant and opossum) showed that the miR-27a binding site is significantly conserved across these mammalian species (Fig.2C). We selected three rodent models of metabolic syndrome to investigate the expression pattern of *Hmgcr* and miR-27a/b levels: BPH *vs*. BPL mice, SHR *vs*. WKY rats and rats fed with high fructose and fat diet (HFHF) *vs*. rats fed with normal chow diet; all these models show altered serum lipid profiles as compared to their controls indicating deregulation of cholesterol homeostasis [(Mouse Phenome Database, Jackson Laboratory; www.jax.org/phenome, The Rat Genome Database (RGD); http://rgd.mcw.edu and (37)]. Interestingly, miR-27a expression in liver tissues showed an inverse correlation with Hmgcr levels in all these models (*SI Appendix*, Fig.S1) while miR-27b levels were

not negatively correlated to Hmgcr expression (*SI Appendix*, Fig.S2). Moreover, miR-27a also showed a significant negative correlation with *Hmgcr* expression in cultured AML12 cells and mouse neuroblastoma N2a cells as well as rat liver, kidney and skeletal muscle tissues (Fig.2B) suggesting it as a promising candidate for further studies. In addition, ectopic expression of miR-27b did not cause any significant change in the m*Hmgcr* 3'UTR reporter activity (*SI Appendix*, Fig.S3A). This is consistent with previous reports where miR-27b mimic caused no significant change in the mRNA levels of HMGCR in hepatocytes (38, 39).

Pathophysiological implications of Hmgcr regulation by miR-27a.

HMGCR is tightly regulated by sterols at multiple levels by transcriptional, post-transcriptional and post-translational mechanisms (as reviewed in (40, 41)). In brief, elevated sterols diminish *HMGCR* expression by inhibiting of Sterol Regulatory Element Binding Protein 2 (SREBP-2) transcription factor (42, 43). The post-transcriptional and post-translational regulatory systems operate independent of SREBP pathway and form an important aspect of sterol-mediated HMGCR regulation. Post-translational regulation is executed by sterol or non-sterol intermediates via INSIG dependent ER-associated protein degradation (ERAD) mechanism involving ubiquitin-proteosomal degradation of HMGCR (43, 44). However, the effect of elevated sterols on miRNA-mediated regulation of *HMCGR* is partially understood. In view of crucial role of sterols in HMCGR regulation, do enhanced cholesterol levels modulate endogenous miR-27a levels? Indeed, exogenous cholesterol treatment to AML12 cells enhanced miR-27a levels as well as diminished Hmgcr protein levels (Fig.5). In order to rule out the possibility that this repression in Hmgcr protein levels is solely because of INSIG-mediated ERAD mechanism, we performed RIP assays in AML12 cells treated with cholesterol. Our RIP assays using anti-Ago2 antibodies further confirmed enhanced interaction of miR-27a with *HMGCR* under elevated cholesterol level suggesting that post-transcriptional regulation of Hmgcr by miR-27a is an additional mechanism for down-regulation of Hmgcr levels under high cholesterol conditions. Moreover, qPCR analyses in liver tissues of rats fed with a high fructose and high fat diet indicate altered miR-27a expression (*SI Appendix*, Fig.S1C). This is reminiscent of multiple studies showing

modulation of miR-27a expression in rodents fed with a high-fat diet (38, 45). Of note, circulating levels of miR-27a were also diminished in subjects with hypercholesterolemia or hypertension (46). Thus, this study revealed the crucial role of intracellular cholesterol on Hmgcr expression via miR-27a.

Are there other microRNAs that modulate lipid or lipoprotein synthesis/secretion into the circulation? There are limited reports on regulatory roles of miRNAs in cholesterol homeostasis. miR-122 inhibition in normal mice results in diminished plasma cholesterol and triglyceride levels as well as reduced fatty acid and cholesterol synthesis (47). Interestingly, deletion of miR-122 in mice causes enhanced hepatic lipid, plasma alanine aminotransferase and alkaline phosphatase levels with the development of steatohepatitis, fibrosis and hepatocellular carcinoma (HCC) with age (48). Likewise, over-expression of miR-34 in mice reduced plasma triglyceride and cholesterol levels but augmented hepatic triglyceride levels causing hepatosteatosis (49). Recent studies indicate miR-30c lowers plasma cholesterol in different mice models of atherosclerosis, hypercholesterolemia and metabolic disorders without increasing plasma transaminases or causing hepatic steatosis (50, 51).

For validation of our *in vitro* findings, we tested the effect of miR-27a mimic in high cholesterol diet-fed *Apoe*$^{-/-}$ mice. As lentiviral delivery of miR-27a would be challenging for therapeutic applications, we report the use of a synthetic miR-27a mimic for this study. Moreover, an improved lipid-based formulation was employed for the efficient delivery of the miR-27a mimic via tail vein injection to major organs viz. the liver, heart and adipose tissues as confirmed by the tissue analysis of miR-27a levels (Fig.7B). Administration of miR-27a over a period of 11 days induced a significant reduction in the plasma total, LDL, cholesterol and triglyceride levels with a concomitant increase in the HDL cholesterol levels (Fig.7E, F, G and H).

miR-27a appears to reduce the plasma cholesterol levels by reducing the Hmgcr mRNA and protein levels in the liver (Fig.7C). The reductions in the plasma triglycerides are consistent with a previous report where miR-27a expression diminished the triglyceride levels in mouse primary hepatocytes mainly by targeting lipogenesis associated genes viz. fatty acid synthase (*Fas*) and stearyl CoA desaturase 1 (*Scd1*) (52). We speculate that the increase in plasma HDL cholesterol levels might result from

the regulation of Scavenger Receptor Class B Member1 (Scarb1), an important membrane receptor for HDL cholesterol (*SI Appendix*, Fig.S9B). Interestingly, ultrasound imaging of the left ventricle and aortic arch revealed improved cardiac function and diminished atherosclerotic lesions in the aortic arches in the miR-27a group as compared to the control group (Fig.8). Histological analyses of the liver sections demonstrate improved liver architecture with diminished lipid accumulation and fibrotic deposition in the miR-27a group in comparison to the control group (Fig.8) suggesting alleviated hepatic steatosis.

Does the miR-27a mimic treatment cause any adverse effects in the diet-induced atherosclerosis mouse model? We did not detect any significant changes in the plasma ALT, AST and CK levels suggesting that the animals did not suffer from any liver or muscle injury (Fig.7I, J and K). However, additional studies are required to test the long-term effects of the miR-27a mimic to further evaluate its therapeutic potential.

Molecular mechanisms of Hmgcr regulation by miR-27a.

miRNAs silence their targets by either translational repression or mRNA degradation. Generally, miRNAs exert their action by translational inhibition followed by mRNA deadenylation, decapping and decay (53). Of late, accumulating evidence suggests that miRNA-mediated mRNA repression can be seen even without the necessity of transcript degradation (54-56). Our actinomycin D chase experiments showed that the Hmgcr mRNA half-life did not change whereas the Hmgcr protein level diminished in a time-dependent manner (Fig.9). Consistently, the steady-state mRNA level of Hmgcr in hepatocytes did not diminish upon over-expression of miR-27a (*SI Appendix*, Fig.S8) suggesting that the mechanism of miR-27a-mediated Hmgcr repression involved translational control.

In view of the key role of miR-27a in regulating Hmgcr we sought to unravel how miR-27a might be regulated under basal and pathophysiological conditions. A series of computational and experimental analyses suggested, for the first time to our knowledge, a crucial role of Egr1 in the activation of miR-27a expression. Egr1, a zinc finger transcription factor belonging to the early growth response gene family, binds to a GC-rich consensus region, GCG(T/G)GGGGG (57) and influences a variety of target genes

involved in physiological stress response, cell metabolism, proliferation and inflammation (58). Egr1 has also been implicated in various cardiovascular pathological processes including atherosclerosis, cardiac hypertrophy and angiogenesis (59). Among the Egr family of genes, Egr1 is pre-dominantly expressed in the liver as well as liver-derived cell lines and targets multiple cholesterol biosynthesis genes (32, 60). In light of computational prediction of multiple Egr1 binding sites in the proximal miR-27a promoter domain (Fig.6A), we investigated the role of Egr1 in miR-27a expression. Indeed, over-expression/down-regulation of Egr1 resulted in enhanced/diminished miR-27a promoter activity in AML12 cells (Fig.6B, C). Consistent with the computational predictions, ChIP analyses confirmed the *in vivo* interaction of Egr1 with the miR-27a promoter (Fig.6F). This is in corroboration with a previous study that reported Egr1 down-regulation attenuates miR-27a expression in human pulmonary artery endothelial cells (61).

Role of miR-27a in global regulation of cholesterol homeostasis.

miR-27a, an intergenic miRNA, is transcribed from the miR-23a-miR-27a-miR-24 cluster located on chromosome 8 in mice. Dysregulation of miR-27a has been associated with several cardiovascular phenotypes including impaired left ventricular contractility, hypertrophic cardiomyopathy, adipose hypertrophy and hyperplasia (62). miR-27a has been reported to regulate several genes involved in adipogenesis and lipid metabolism including Retinoid X receptor alpha (RXRα), ATP-binding cassette transporter (ABCA1) also known as the cholesterol efflux regulatory protein, fatty acid synthase (FASN), sterol regulatory element-binding proteins (SREBP-1 and -2), peroxisome proliferator-activated receptor (PPAR-α and -γ), Apolipoprotein A-1, Apolipoprotein B-100 and Apolipoprotein E-3 [as reviewed in (30)]. In addition, miR-27a has been reported to play a role in the regulation of low density lipoprotein receptor (*Ldlr)* (63). Our *in vitro* and *in vivo* experiments revealed that miR-27a targets *Mvk*, *Fdft1*, *Sqle*, *Ggps1* and *Mvd* in the cholesterol biosynthesis pathway (Fig.10). Consistent with our findings, administration of miR-27a mimic in *Apoe*$^{-/-}$ mice diminished lipid levels in both plasma and peritoneal macrophages mainly by targeting macrophage-derived lipoprotein lipase (Lpl), a crucial ligand for receptor mediated-lipoprotein uptake (64). Of note, HITS-CLIP experiments

revealed that miR-27a also targeted microsomal triglyceride transfer protein (Mttp), a crucial chaperone involved in lipoprotein production and a promising target for lowering plasma lipids (50, 51, 65). Further, global pathway analysis for miR-27a targets revealed 21 pathways including fatty acid and steroid biosynthesis (*SI Appendix*, Fig.S10). These findings are in line with an *in silico* miR-27a/b target prediction report (66). Thus, miR-27a contributes to global regulation of cholesterol homeostasis by targeting multiple genes in lipid synthesis, lipoprotein synthesis as well as lipoprotein uptake.

Limitations of the study.

Although our findings indicate that miR-27a mimic effectively lowers plasma cholesterol levels and atherosclerosis, there are some challenges that remain unaddressed. First, a less-/non-invasive method of delivery (viz. subcutaneous or oral route) over intravenous injections would be desirable for easy administration of the mimic. Second, improved lipid formulations or nanoparticle-mediated delivery would considerably reduce the amount of mimic required and eliminate the need for frequent injections. Additionally, further chemical modifications to this mimic may attribute to increased target specificity and resistance to nuclease activity. Moreover, extensive assessment of biological and pharmacological effects of miR-27a mimic in animal models are necessary to evaluate its long-term safety and efficacy as a therapeutic agent.

Conclusions and perspectives.

This study identified miR-27a as a crucial regulator of cholesterol biosynthesis pathway. Egr1 mediates the regulation of Hmgcr by miR-27a under basal and elevated cholesterol conditions. miR-27a directly interacts with the 3'-UTR of Hmgcr mRNA and represses Hmgcr protein level by translational attenuation. Augmentation of miR-27a in *Apoe*$^{-/-}$ mice diminished the plasma lipid levels and attenuated the progression of atherosclerosis. These findings provide novel insights on the plausible role of miR-27a in the post-transcriptional regulation of Hmgcr, thereby implicating its role in cholesterol homeostasis under pathophysiological conditions.

miRNA therapeutics is an emerging and promising avenue to treat a wide array of human diseases. A fine balance between lipid/lipoprotein synthesis and lipoprotein uptake is essential for cholesterol homeostasis and dysregulation of any one pathway could lead to drastic effects. Therefore, miRNAs targeting multiple related pathways may be more efficacious in lowering plasma lipids than the conventional approach of targeting individual proteins/pathways. In view of the ability of miR-27a to target several crucial genes in the cholesterol biosynthesis pathway, miR-27a mimic emerges as a promising therapeutic intervention to lower plasma cholesterol and atherosclerosis. Our findings and other studies provide strong impetus for further preclinical studies and subsequent human trials for miR-27a as a novel lipid-lowering agent.

MATERIALS AND METHODS.

The detailed methodologies are included in the *SI Appendix, SI Materials and Methods*.

Comparative genomics analyses.

For comparative genomic analysis, the data pertaining to lipid-related QTLs, their respective LOD scores, and all the genes with their respective positions in a particular QTL was mined from the Rat Genome Database (*SI Appendix*, Table S2). We also compared the mouse and rat *Hmgcr* gene sequences (GenBank accession no: NM_008255, and NM_ NM_013134.2, respectively) retrieved from UCSC genome browser (http://www.genome.ucsc.edu/) using mVISTA browser.

In silico predictions of potential miRNA binding sites in *Hmgcr*-3′UTR and putative miRNA targets in the cholesterol biosynthesis pathway.

Mouse Hmgcr (*Hmgcr*)-3'UTR sequence (NCBI reference number: NM_008255.2) was downloaded from the UCSC genome browser and analyzed using multiple bioinformatic algorithms [viz. miRWalk, miRanda, TargetScan, PITA, RNA22 and RNAhybrid (*SI Appendix*, Table S2)] to predict miRNA target sites. Putative mouse miR-27a target genes were retrieved from TargetScan, RNAhybrid and miRWalk (*SI Appendix*, Table S2). These datasets were used as input for the PANTHER classification system (http://www.pantherdb.org/) which grouped them based on their molecular functions and gene IDs that mapped to the cholesterol biosynthesis pathway were selected.

Tissue-specific expression of endogenous *HMGCR* and hsa-miR-27a-3p levels.

HMGCR expression data in various human tissues was mined from the GTEx portal (*SI Appendix*, Table S2). Likewise, tissue-specific hsa-miR-27a-3p expression was obtained from miRmine and DASHR (*SI Appendix*, Table S2), respectively. Only tissues common to the GTEx portal and DASHR or miRmine were chosen for correlation analysis. The data was normalized to a particular tissue in each set of analysis and expressed as fold change. In brief, the expression data from miRmine and GTEx was normalized to pancreas while the expression in spleen was used for normalizing expression profiles from DASHR.

Generation of *Hmgcr* 3'-UTR/luciferase, mmu-miR-27a promoter/luciferase reporter constructs and miRNA expression plasmids.

The mouse *Hmgcr* 3'-UTR domain (+20359/+21975 bp) was PCR-amplified and cloned in pGL3-promoter reporter vector (Promega). To generate the mmu-miR-27a promoter/luciferase reporter construct, -1079 bp to +26 bp region of the miR-27a promoter was PCR-amplified using mouse genomic DNA and cloned in pGL3-basic vector (Promega). miR-27a and miR-27b expression plasmids were generated in pcDNA3.1 vector (Invitrogen).

Cell lines, transfections and reporter assays.

AML12, N2a and HuH-7 cells were cultured and transfected/treated under various conditions as detailed in *SI Appendix, SI Materials and Methods*. Reporter assays were carried out as described previously (67, 68).

Animals and tissue samples.

All animal-related procedures were approved by the Institutional Animal Ethics Committee at Indian Institute of Technology Madras and described in *SI Appendix, SI Materials and Methods*.

Analysis of biochemical parameters in plasma, blood and tissue samples from the miRNA/ control oligo-treated mice.

The plasma total, HDL, LDL cholesterol, ALT (alanine aminotransferase), AST (aspartate aminotransferase) and CK (creatine kinase) levels were measured using commercial kits (Randox) as per manufacturer's instructions. For hepatic cholesterol estimations, lipids were extracted from liver tissue and tissue total cholesterol was assayed by Amplex Red cholesterol assay kit (Thermo Fisher). The fasting blood glucose levels were measured using an Accu-Chek Active Blood Glucometer.

Ultrasound imaging, aortic plaque and histopathological analyses.

Transthoracic echocardiography and ultrasound imaging of the aortic arch was performed on all the experimental animals before and after the miR-27a mimic/control

oligo injections using a Vevo High resolution ultrasound imaging system (VisualSonics) with an MS400 scan head (30 MHz) as previously described (69, 70). Plaque burden was assessed by measuring vessel wall thickness at the lesser curvature of the arch.

For analyzing aortic plaques, the aortic arches were dissected and exposed after carefully removing the fat and connective tissue around the heart and the aorta. Photographs of the exposed aortic arches were taken by a dissecting microscope (Nikon, C-FLED2). For microscopic examination, liver tissues were stained with hematoxylin-eosin (H&E). Liver fibrosis was assessed by Picro Sirius Red (PSR) staining. Oil red O staining was performed in liver tissue sections to assess lipid content as described previously (71).

RNA extraction and Real-time PCR.

Total RNA extracted from cell lines and tissue samples was subjected to cDNA synthesis using High Capacity cDNA Reverse Transcription Kit (Applied Biosystems) and miR-27a/miR-27b/U6-specific stem-loop (SL; *SI Appendix*, Table S1) or random hexamer primers. Quantitative Real-time PCR (qPCR) was performed using miRNA specific primers and a universal reverse primer or gene specific primers (*SI Appendix*, Table S1). In all the qPCR analysis, the relative abundance of miR-27a and *Hmgcr* was determined by calculating $2^{-\Delta\Delta Ct}$ of each reaction (72).

Filipin staining of hepatocyte cells.

AML12 cells treated with 20 µg/ml of exogenous cholesterol or 5mM of cholesterol-depleting reagent methyl-β-cyclodextrin (MCD) were fixed, stained with 50 µg/ml of Filipin III (a fluorescent dye that binds to free cholesterol) and imaged using an Olympus U-RFL-T fluorescence microscope (Olympus, Japan).

mRNA stability assays.

Actinomycin D chase experiments were carried out to determine the Hmgcr mRNA stability as described earlier (73) The Hmgcr mRNA half-life from three different experiments was averaged and standard error calculated.

Ago2-Ribonucleoprotein immunoprecipitation (RIP) assays.

To probe the endogenous interaction of miR-27a with *Hmgcr*, Ago2-RIP experiments were carried out as described previously (74)

Western Blot Analysis.

Up-regulation or down-regulation of Hmgcr/HMGCR⁄Egr1 after transfection experiments/cholesterol treatment/ depletion was determined by Western blotting.

Chromatin Immunoprecipitation (ChIP) Assays.

ChIP assays were performed to confirm the interaction of Egr1 with the miR-27a promoter *in vivo* in the context of chromatin and mentioned in *SI Appendix, SI Materials and Methods*.

Data presentation and Statistical analysis.

All 3'UTR-reporter/promoter-reporter transient transfection experiments were carried out at least three times and results were expressed as mean ± SEM of triplicates from representative experiments. Prism 5 program (GraphPad Software, San Diego, CA, USA) was used to determine the level of statistical significance by Student's t-test or one-way ANOVA with Newman-Keuls's post-test, as appropriate.

Acknowledgements

This work was supported by a grant from the Council of Scientific and Industrial Research (CSIR), Government of India to NRM (project number: 37(1564)/12-EMR-II). This work was also supported by an Exploratory Research Project grant from Industrial Consultancy & Sponsored Research, IIT Madras. Research fellowships were received from Ministry of Human Resource Development (to AAK and VG), Department of Science and Technology (to VA), Indian Council of Medical Research (to SSR and HA), CSIR (to AK), Government of India. The authors are grateful to Dr. Dona Lee Wong (Harvard Medical School, Boston) for providing us with the Egr1 expression plasmid, and to Dr. Weihua Xiao (University of Science and Technology of China, Hefei) for the Egr1-shRNA plasmid.

REFERENCES

1. Benjamin EJ*, et al.* (2018) Heart Disease and Stroke Statistics-2018 Update A Report From the American Heart Association. *Circulation* 137(12):E67-E492.
2. Sathiyakumar V*, et al.* (2018) Novel Therapeutic Targets for Managing Dyslipidemia. *Trends Pharmacol Sci* 39(8):733-747.
3. Athyros VG*, et al.* (2018) Diabetes and lipid metabolism. *Hormones* 17(1):61-67.
4. Palacio Rojas M*, et al.* (2017) Dyslipidemia: Genetics, lipoprotein lipase and HindIII polymorphism. *F1000Res* 6:2073.
5. Geelen MJH, Gibson DM, & Rodwell VW (1986) Hydroxymethylglutaryl-CoA reductase--the rate-limiting enzyme of cholesterol biosynthesis. A report of a meeting held at Nijenrode Castle, Breukelen, The Netherlands, August 24, 1985. *FEBS Lett* 201(2):183-186.
6. Goldstein JL & Brown MS (1990) Regulation of the Mevalonate Pathway. *Nature* 343(6257):425-430.
7. DeBose-Boyd RA (2008) Feedback regulation of cholesterol synthesis: sterol-accelerated ubiquitination and degradation of HMG CoA reductase. *Cell Res* 18(6):609-621.
8. Stone NJ*, et al.* (2014) 2013 ACC/AHA guideline on the treatment of blood cholesterol to reduce atherosclerotic cardiovascular risk in adults: a report of the American College of Cardiology/American Heart Association Task Force on Practice Guidelines. *J Am Coll Cardiol* 63(25):2889-2934.
9. Watts GF*, et al.* (2014) Integrated guidance on the care of familial hypercholesterolaemia from the International FH Foundation. *Int J Cardiol* 171(3):309-325.
10. Kathiresan S*, et al.* (2008) Six new loci associated with blood low-density lipoprotein cholesterol, high-density lipoprotein cholesterol or triglycerides in humans. *Nat Genet* 40(2):189-197.
11. Aulchenko YS*, et al.* (2009) Loci influencing lipid levels and coronary heart disease risk in 16 European population cohorts. *Nat Genet* 41(1):47-55.
12. Burkhardt R*, et al.* (2008) Common SNPs in HMGCR in micronesians and whites associated with LDL-cholesterol levels affect alternative splicing of exon13. *Arterioscler Thromb Vasc Biol* 28(11):2078-2084.
13. Hiura Y*, et al.* (2010) Association of the functional variant in the 3-hydroxy-3-methylglutaryl-coenzyme a reductase gene with low-density lipoprotein-cholesterol in Japanese. *Circ J* 74(3):518-522.
14. Freitas RN*, et al.* (2009) A HMGCR polymorphism is associated with relations between blood pressure and urinary sodium and potassium ratio in the Epic-Norfolk Study. *J Am Soc Hypertens* 3(4):238-244.
15. Freitas RN*, et al.* (2010) HMGCR gene polymorphism is associated with stroke risk in the EPIC-Norfolk study. *Eur J Cardiovasc Prev Rehabil* 17(1):89-93.
16. Luo H*, et al.* (2017) Genetic variants influencing lipid levels and risk of dyslipidemia in Chinese population. *J Genet* 96(6):985-992.
17. Swerdlow DI*, et al.* (2015) HMG-coenzyme A reductase inhibition, type 2 diabetes, and bodyweight: evidence from genetic analysis and randomised trials. *Lancet* 385(9965):351-361.

18. Krauss RM*, et al.* (2008) Variation in the 3-hydroxyl-3-methylglutaryl coenzyme a reductase gene is associated with racial differences in low-density lipoprotein cholesterol response to simvastatin treatment. *Circulation* 117(12):1537-1544.
19. Medina MW, Gao F, Ruan W, Rotter JI, & Krauss RM (2008) Alternative splicing of 3-hydroxy-3-methylglutaryl coenzyme A reductase is associated with plasma low-density lipoprotein cholesterol response to simvastatin. *Circulation* 118(4):355-362.
20. Thompson JF*, et al.* (2009) Comprehensive whole-genome and candidate gene analysis for response to statin therapy in the Treating to New Targets (TNT) cohort. *Circ Cardiovasc Genet* 2(2):173-181.
21. Zhang C (2008) MicroRNomics: a newly emerging approach for disease biology. *Physiol Genomics* 33(2):139-147.
22. Krutzfeldt J & Stoffel M (2006) MicroRNAs: a new class of regulatory genes affecting metabolism. *Cell Metab* 4(1):9-12.
23. Thum T, Catalucci D, & Bauersachs J (2008) MicroRNAs: novel regulators in cardiac development and disease. *Cardiovasc Res* 79(4):562-570.
24. Najafi-Shoushtari SH (2011) MicroRNAs in cardiometabolic disease. *Curr Atheroscler Rep* 13(3):202-207.
25. Chang TC & Mendell JT (2007) microRNAs in vertebrate physiology and human disease. *Annu Rev Genomics Hum Genet* 8:215-239.
26. Nemecz M, Alexandru N, Tanko G, & Georgescu A (2016) Role of MicroRNA in Endothelial Dysfunction and Hypertension. *Curr Hypertens Rep* 18(12):87.
27. Condorelli G, Latronico MVG, & Cavarretta E (2014) microRNAs in cardiovascular diseases: current knowledge and the road ahead. *J Am Coll Cardiol* 63(21):2177-2187.
28. Peters LL*, et al.* (2007) The mouse as a model for human biology: a resource guide for complex trait analysis. *Nat Rev Genet* 8(1):58-69.
29. Alexiou P, Maragkakis M, Papadopoulos GL, Reczko M, & Hatzigeorgiou AG (2009) Lost in translation: an assessment and perspective for computational microRNA target identification. *Bioinformatics* 25(23):3049-3055.
30. Yang Z, Cappello T, & Wang L (2015) Emerging role of microRNAs in lipid metabolism. *Acta Pharm Sin B* 5(2):145-150.
31. Zidovetzki R & Levitan I (2007) Use of cyclodextrins to manipulate plasma membrane cholesterol content: evidence, misconceptions and control strategies. *Biochim Biophys Acta* 1768(6):1311-1324.
32. Gokey NG, Lopez-Anido C, Gillian-Daniel AL, & Svaren J (2011) Early growth response 1 (Egr1) regulates cholesterol biosynthetic gene expression. *J Biol Chem* 286(34):29501-29510.
33. Golomb BA & Evans MA (2008) Statin adverse effects : a review of the literature and evidence for a mitochondrial mechanism. *Am J Cardiovasc Drugs* 8(6):373-418.
34. Singh AK*, et al.* (2018) Posttranscriptional regulation of lipid metabolism by non-coding RNAs and RNA binding proteins. *Semin Cell Dev Biol* 81:129-140.
35. van Rooij E & Kauppinen S (2014) Development of microRNA therapeutics is coming of age. *EMBO Mol Med* 6(7):851-864.

36. Selitsky SR*, et al.* (2015) Transcriptomic Analysis of Chronic Hepatitis B and C and Liver Cancer Reveals MicroRNA-Mediated Control of Cholesterol Synthesis Programs. *MBio* 6(6):e01500-01515.
37. Saravanan N, Patil MA, Kumar PU, Suryanarayana P, & Reddy GB (2017) Dietary ginger improves glucose dysregulation in a long-term high-fat high-fructose fed prediabetic rat model. *Indian J Exp Biol* 55(3):142-150.
38. Vickers KC*, et al.* (2013) MicroRNA-27b is a regulatory hub in lipid metabolism and is altered in dyslipidemia. *Hepatology* 57(2):533-542.
39. Goedeke L*, et al.* (2015) miR-27b inhibits LDLR and ABCA1 expression but does not influence plasma and hepatic lipid levels in mice. *Atherosclerosis* 243(2):499-509.
40. Brown MS & Goldstein JL (2009) Cholesterol feedback: from Schoenheimer's bottle to Scap's MELADL (vol 50, pg S15, 2009). *J Lipid Res* 50(6):1255-1255.
41. Sharpe LJ, Cook EC, Zelcer N, & Brown AJ (2014) The UPS and downs of cholesterol homeostasis. *Trends Biochem Sci* 39(11):527-535.
42. Horton JD, Goldstein JL, & Brown MS (2002) SREBPs: activators of the complete program of cholesterol and fatty acid synthesis in the liver. *J Clin Invest* 109(9):1125-1131.
43. Brown AJ, Sun L, Feramisco JD, Brown MS, & Goldstein JL (2002) Cholesterol addition to ER membranes alters conformation of SCAP, the SREBP escort protein that regulates cholesterol metabolism. *Mol Cell* 10(2):237-245.
44. Song BL & DeBose-Boyd RA (2004) Ubiquitination of 3-hydroxy-3-methylglutaryl-CoA reductase in permeabilized cells mediated by cytosolic E1 and a putative membrane-bound ubiquitin ligase. *J Biol Chem* 279(27):28798-28806.
45. Alisi A*, et al.* (2011) Mirnome analysis reveals novel molecular determinants in the pathogenesis of diet-induced nonalcoholic fatty liver disease. *Lab Invest.* 91(2):283-293.
46. Karolina DS*, et al.* (2012) Circulating miRNA profiles in patients with metabolic syndrome. *J Clin Endocrinol Metab.* 97(12):E2271-E2276.
47. Esau C*, et al.* (2006) miR-122 regulation of lipid metabolism revealed by in vivo antisense targeting. *Cell Metab* 3(2):87-98.
48. Tsai WC*, et al.* (2012) MicroRNA-122 plays a critical role in liver homeostasis and hepatocarcinogenesis. *J Clin Invest* 122(8):2884-2897.
49. Xu Y*, et al.* (2015) A metabolic stress-inducible miR-34a-HNF4alpha pathway regulates lipid and lipoprotein metabolism. *Nat Commun* 6:7466.
50. Irani S, Iqbal J, Antoni WJ, Ijaz L, & Hussain MM (2018) microRNA-30c reduces plasma cholesterol in homozygous familial hypercholesterolemic and type 2 diabetic mouse models. *J Lipid Res* 59(1):144-154.
51. Irani S*, et al.* (2016) MicroRNA-30c Mimic Mitigates Hypercholesterolemia and Atherosclerosis in Mice. *J Biol Chem* 291(35):18397-18409.
52. Zhang MY, Sun WL, Zhou MH, & Tang Y (2017) MicroRNA-27a regulates hepatic lipid metabolism and alleviates NAFLD via repressing FAS and SCD1. *Sci Rep* 7.
53. Nishimura T & Fabian MR (2016) Scanning for a unified model for translational repression by microRNAs. *EMBO J* 35(11):1158-1159.

54. Bazzini AA, Lee MT, & Giraldez AJ (2012) Ribosome profiling shows that miR-430 reduces translation before causing mRNA decay in zebrafish. *Science* 336(6078):233-237.
55. Ferland-McCollough D*, et al.* (2012) Programming of adipose tissue miR-483-3p and GDF-3 expression by maternal diet in type 2 diabetes. *Cell Death Differ.* 19(6):1003-1012.
56. Daimiel-Ruiz L*, et al.* (2015) Dietary lipids modulate the expression of miR-107, a miRNA that regulates the circadian system. *Mol Nutr Food Res.* 59(9):1865-1878.
57. Christy B & Nathans D (1989) DNA binding site of the growth factor-inducible protein Zif268. *Proc Natl Acad Sci U S A* 86(22):8737-8741.
58. Fu M*, et al.* (2003) Egr-1 target genes in human endothelial cells identified by microarray analysis. *Gene* 315:33-41.
59. Khachigian LM (2006) Early growth response-1 in cardiovascular pathobiology. *Circ Res* 98(2):186-191.
60. Mohn KL, Laz TM, Melby AE, & Taub R (1990) Immediate-early gene-expression differs between regenerating liver, insulin-stimulated H-35 cells, and mitogen-stimulated Balb/C 3t3 Cells. Liver-specific induction-patterns of gene-33, phosphoenolpyruvate carboxykinase, and the jun, fos, and egr families. *J Biol Chem.* 265(35):21914-21921.
61. Kang BY*, et al.* (2013) Hypoxia mediates mutual repression between microRNA-27a and PPARgamma in the pulmonary vasculature. *PLoS One* 8(11):e79503.
62. Devaux Y*, et al.* (2013) A panel of 4 microRNAs facilitates the prediction of left ventricular contractility after acute myocardial infarction. *PLoS One* 8(8):e70644.
63. Alvarez ML, Khosroheidari M, Eddy E, & Done SC (2015) MicroRNA-27a decreases the level and efficiency of the LDL receptor and contributes to the dysregulation of cholesterol homeostasis. *Atherosclerosis* 242(2):595-604.
64. Xie W*, et al.* (2016) MicroRNA-27 Prevents Atherosclerosis by Suppressing Lipoprotein Lipase-Induced Lipid Accumulation and Inflammatory Response in Apolipoprotein E Knockout Mice. *PLoS One* 11(6):e0157085.
65. Schug J*, et al.* (2013) Dynamic recruitment of microRNAs to their mRNA targets in the regenerating liver. *BMC Genomics* 14.
66. Chen WJ, Yin K, Zhao GJ, Fu YC, & Tang CK (2012) The magic and mystery of microRNA-27 in atherosclerosis. *Atherosclerosis* 222(2):314-323.
67. Mahapatra NR*, et al.* (2006) Molecular basis of neuroendocrine cell type-specific expression of the chromogranin B gene: Crucial role of the transcription factors CREB, AP-2, Egr-1 and Sp1. *J Neurochem* 99(1):119-133.
68. Mahapatra NR, Mahata M, O'Connor DT, & Mahata SK (2003) Secretin activation of chromogranin A gene transcription. Identification of the signaling pathways in cis and in trans. *J Biol Chem* 278(22):19986-19994.
69. Reddy SS, Agarwal H, & Barthwal MK (2018) Cilostazol ameliorates heart failure with preserved ejection fraction and diastolic dysfunction in obese and non-obese hypertensive mice. *J Mol Cell Cardiol* 123:46-57.
70. Kaufmann BA*, et al.* (2010) Molecular Imaging of the Initial Inflammatory Response in Atherosclerosis Implications for Early Detection of Disease. *Arterioscl Throm Vas* 30(1):54-U132.

71. Hu YW*, et al.* (2016) VNN1 promotes atherosclerosis progression in apoE(-/-) mice fed a high-fat/high-cholesterol diet. *J Lipid Res* 57(8):1398-1411.
72. Livak KJ & Schmittgen TD (2001) Analysis of relative gene expression data using real-time quantitative PCR and the 2(-Delta Delta C(T)) Method. *Methods* 25(4):402-408.
73. Dolken L*, et al.* (2008) High-resolution gene expression profiling for simultaneous kinetic parameter analysis of RNA synthesis and decay. *RNA* 14(9):1959-1972.
74. Tan LP*, et al.* (2009) A high throughput experimental approach to identify miRNA targets in human cells. *Nucleic Acids Res* 37(20):e137.

Table 1: A list of predicted miRNAs having potential binding sites in the 3'-UTR of m*Hmgcr

miRNA	Seed sequence (No. of bases)	ΔΔG (PITA)	RNAhybrid ΔG (kcal/mol)
mmu-miR-124	7	-10.62	-29.5
mmu-miR-28	8	-10.28	-22.2
mmu-miR-345-5p	8	-11.08	-32
mmu-miR-351	8	-16.89	-33.6
mmu-miR-708	7	-14.34	-27.4
mmu-miR-27a	6	-10.13	-20.7
mmu-miR-27b	6	-10.74	-22.6

* miRNAs predicted by atleast 5 programs that displayed a PITA ΔΔG score of less than -10 and RNAhybrid ΔG value of -20 kcal/mol were selected

Table 2 Genomic position and LOD score of various lipid/cholesterol QTLs present on rat chromosome 2 (26000000- 28000000 bp) *

Blood Pressure QTLs	Start position (bp)	Stop position (bp)	LOD Score
Stl32	22612952	67612952	3.2
Stl27	23837491	149614623	4.4
Scl55	26186097	142053534	2.83
Sffal3	27760301	72760301	6.78
Scl17	228712271	266435125	3.4
Scl8	231621666	266435125	4.4

*This data was retrieved from Rat genome database (http://rgd.mcw.edu/rgdweb/search/qtls.html?100).

FIGURE LEGENDS

Fig.1. Graphical representation of rat QTLs contributing to elevated lipid/cholesterol levels and homology between mouse- and rat-*Hmgcr* gene sequences. (A)The lipid/cholesterol-QTLs and their respective LOD scores (retrieved from Rat Genome Database) were plotted. Three of these six QTLs harbor the *Hmgcr* gene. The genomic position of rat *Hmgcr* gene is indicated. (B) Conservation analysis of rat and mouse *Hmgcr* sequences was performed using mVISTA. The horizontal axis represents the rat *Hmgcr* gene (chr2: 27480226- 27500654) as the reference sequence, whereas the vertical axis indicates the percentage homology between rat and mouse *Hmgcr* gene (chr13: 96,650,579-96,666,685). Here, window size (length of comparison) was set to 100 bp with a minimum of 70% match. Both the mouse and rat *Hmgcr* genes comprise of twenty exons; 5'-UTRs are not visible in the homology plot due to their very small sizes. CNS: conserved non-coding sequences; UTR: untranslated region.

Fig.2. miR-27a binding sites in the 3'-UTR of *Hmgcr* and inverse correlation between mmu-miR-27a-3p/hsa-miR-27a-3p and *Hmgcr/HMGCR* expression. (A) Schematic representation of the *Hmgcr* gene showing the miR-27a binding site in the 3'-UTR. The complementarity between the seed region of miR-27a and mHmgcr-3'UTR is depicted in bold and capital. Positions of the transcription initiation/cap site (indicated as +1 bp), 5'-UTR, exons and 3'-UTR are also shown. **(B)** Negative correlation between *Hmgcr* mRNA and miR-27a expression in cultured AML12, N2a cells, rat liver, kidney and skeletal muscle tissues**.** RNA and miRNAs isolated from the aforementioned cells and tissues were probed for *Hmgcr* and miR-27a expression by qPCR. *Hmgcr* mRNA and miR-27a expressions were normalized to mouse β-actin mRNA and U6 RNA in the same sample, respectively. A strong inverse correlation was observed and the Pearson r and p values are indicated. **(C)** The conservation of the miR-27a binding site in the 3'-UTR of *Hmgcr* across different mammals. The seed region along with the mature mmu-miR-27a sequence is shown at the top of the figure. **(D)** Inverse correlation between *HMGCR* and hsa-miR-27a-3p expression in different tissues. Endogenous *HMGCR* expression profiles in different human tissues was obtained from the GTEx portal while

hsa-miR-27a-3p expression data was retrieved from miRmine and DASHR, respectively. Only tissues common to the GTEx portal and DASHR or miRmine were chosen for correlation analysis and the expression is represented as fold change (when normalized to pancreas for miRmine and spleen for DASHR). The Pearson r and p values for each database are shown.

Fig.3. miR-27a negatively regulates Hmgcr in AML12 and HuH-7 cells. The m*Hmgcr* 3'UTR reporter construct (500 ng) was co-transfected with increasing doses of miR-27a expression plasmid in (A) AML12, (B) HuH-7 cells and luciferase activity was assayed. Values were normalized to total protein and expressed as percentage fold change over basal. The results are mean ± SEM of triplicate values. AML12 or HuH-7 cells were transfected with increasing doses of miR-27a expression plasmid followed by total RNA isolation and cDNA synthesis. The expression of miR-27a was analyzed by qPCR using miRNA specific primers (*SI Appendix*, Table S1) and miR-27 expression was normalized to U6 RNA. Transfection of miR-27a expression plasmid results in over-expression of miR-27a in (C) AML12 and (D) HuH-7 cells, respectively. Statistical significance was determined by one-way ANOVA with Newman-Keuls multiple comparison test. *p<0.05, **p<0.01, ***p<0.001 as compared to the control (without miRNA-27a over-expression). Down-regulation of Hmgcr was confirmed by Western blot analysis and is shown (C and D).

Fig.4. Specific interaction of miR-27a with *Hmgcr* 3'-UTR. The relative expressions of (A) miR-27a and (B) *Hmgcr* upon transfection of 60 nM of control oligo or locked nucleic acid inhibitor of 27a (LNA27a) in AML12 cells were determined by qPCR using miR-27a/gene-specific primers (*SI Appendix*, Table S1). miR-27a and *Hmgcr* expressions were normalized to U6 RNA and mouse β-actin mRNA in the same sample, respectively. (C) Representative Western blot analysis of Hmgcr protein levels in AML12 cells upon transfection of 60 nM of control oligo or LNA27a. The Hmgcr protein levels are normalized to vinculin and normalized values are indicated below the blots. (D) miR-27a and (E) Hmgcr mRNA levels upon transfection of 1 µg of control oligo or miR-27a mimic in AML12 cells were determined by qPCR using miRNA/gene-specific

primers. (F) Representative Western blot analysis of Hmgcr protein levels in AML12 cells upon transfection of 1 µg of control oligo or miR-27a mimic. The Hmgcr protein levels are normalized to vinculin and normalized values are indicated below the blots. (G) Ribonucleoprotein Ago2 precipitation analysis in HuH-7 cells over-expressing miR-27a. HuH-7 cells were transfected with either pcDNA3.1 (control) or miR-27a expression plasmid. After 30-36 hrs of transfection, miRNA-27a-RISC (RNA-induced silencing complex) complexes were immunoprecipitated with Ago2/ pre-immune anti-mouse IgG antibody and *HMGCR* levels were measured by qPCR using h*Hmgcr* (*HMGCR*) primers (*SI Appendix*, Table S1). The *HMGCR* enrichment was normalized to the corresponding input in each condition; expressed as % input and is mean ± SEM for quadruplets. (H) Immunoprecipitation of Ago2 was confirmed by Western blotting. Ago2 was pulled down when appropriate antibody was used (lanes 5 and 6) while the mouse IgG revealed no immunoprecipitation of Ago2 (lanes 3 and 4). Statistical significance was determined by Student's *t*-test (unpaired, 2-tailed). *p<0.05, **p<0.01 as compared to control.

Fig.5. Intracellular cholesterol modulates the expression of miR-27a and augments the miR-27a interaction with the *Hmgcr* 3'-UTR. AML12 cells were treated with increasing doses of either cholesterol ((3β)-cholest-5-en-3-ol) or cholesterol-depleting reagent methyl-β-cyclodextrin (MCD) for 6 hrs or 15 minutes, respectively. After incubation for 6-9 hrs in serum free media, the cells were processed for RNA, protein isolation and fluorescence microscopy. Western blot analysis of total protein isolated from AML12 cells treated with (A) cholesterol or (B) MCD was carried out for Hmgcr and β-actin levels. miR-27a levels were also determined by qPCR on (C) exogenous cholesterol (20 µg/ml) or (D) MCD (5 mM) treatment in AML12 cells. The miR-27a expression was normalized to U6 RNA and indicated as mean ± SEM for triplicate values. (E) Cholesterol or (F) MCD treatments in AML12 cells were confirmed by staining intracellular cholesterol using Filipin stain followed by fluorescence microscopy. Scale bar: 170 µm. (G and H) Enrichment of *HMGCR* and miR-27a upon exogenous cholesterol treatment in Ago2-immunoprecipitated RNA from HuH-7 cells. HuH-7 cells were treated with 20 µg/ml of cholesterol [(3β)-cholest-5-en-3-ol] for 6 hrs

and the total RNA fraction from the Ago2/IgG-immunoprecipitated samples (in basal and cholesterol-treated cells) was subjected to qPCR using (G) *HMGCR* and (H) miR-27a specific primers (*SI Appendix*, Table S1). The *HMGCR*/miR-27a enrichment was normalized to the corresponding input in each condition and represented as % input. Statistical significance was determined by Student's *t*-test (unpaired, 2-tailed). *p<0.05, **p<0.01 and ***p<0.001 as compared to the basal condition.

Fig.6. Egr1 modulates miR-27a expression under basal and altered cholesterol conditions. (A) Schematic representation of the proximal (~1 kb) mmu-miR-27a promoter domain harboring multiple Egr1 binding sites as predicted by LASAGNA and JASPAR. (B & C) Effect of over-expression/down-regulation of Egr1 on miR-27a promoter activity. AML 12 cells were co-transfected with increasing doses of either (B) Egr1 expression plasmid or (C) Egr1 shRNA expression plasmid and miR-27a promoter construct (500 ng). Results are expressed as mean ± SEM for triplicate values. Statistical significance was determined by one-way ANOVA with Newman-Keuls multiple comparison test. * p<0.05, ****p <0.0001 as compared to the basal miR-27a promoter activity. Over-expression/down-regulation of Egr1 was confirmed by Western blot analysis. AML12 cells were co-transfected with mmu-miR-27a promoter (500 ng) and 500 ng of either (D) Egr1 expression plasmid or (E) Egr1 shRNA expression plasmid followed by qPCR to probe for the endogenous levels of miR-27a (normalized to U6 RNA). Statistical significance was determined by Student's *t*-test (unpaired, 2-tailed). *p<0.05 as compared to the control condition. (F) *In vivo* interaction of Egr1 with miR-27a promoter domain. ChIP assay was carried out using chromatin isolated from AML12 cells. qPCR was performed with DNA purified from respective cocktails using primer pair P2 amplifying 140 bp DNA segment (Egr1 cluster 2) in the proximal miR-27a promoter domain. Statistical significance was determined by Student's *t*-test (unpaired, 2-tailed). *p<0.05 and **p<0.01 as compared to the control. AML12 cells were treated with either (G) 20 µg/ml of cholesterol [(3β)-cholest-5-en-3-ol] or (H) 5 mM of cholesterol-depleting reagent methyl-β-cyclodextrin (MCD) for 6 hrs or 15 minutes, respectively. Western blot analysis of total proteins was carried out probing for Egr1 and vinculin. Relative levels of Egr1 after normalization with vinculin are shown.

Fig.7. miR-27a hinders the progression of atherosclerosis in *Apoe*$^{-/-}$ mice. (A) Male *Apoe*$^{-/-}$ mice (8-10 weeks old) were started on a high-cholesterol diet regimen for a period of 10 weeks and injected with either miR-27a mimic or control oligo twice over a period of 11 days and then euthanized as indicated in the schematic representation. (B) Tissue analysis of miR-27a expression by qPCR using miRNA-specific primers (*SI Appendix*, Table S1). miR-27a expression was normalized to U6 RNA. (C) Western blot analysis of liver tissues for Hmgcr and vinculin protein levels. The Hmgcr protein levels are normalized to vinculin and normalized values are indicated below the blots. (D) Lipids were extracted from liver tissue and hepatic cholesterol levels were measured in control oligo (n=5) and miR-27a-injected *Apoe*$^{-/-}$ mice (n=4). Plasma from overnight-fasted animals was collected prior to sacrificing the animals to measure the plasma (E) total cholesterol, (F) LDL cholesterol, (G) triglycerides, (H) HDL cholesterol, (I) ALT, (J) AST and (K) CK levels (n=5 in each group). Statistical significance was determined by Student's *t*-test (unpaired, 2-tailed). * $p<0.05$, ** $p<0.01$ and *** $p<0.001$ as compared to the control oligo-treated group.

Fig.8. miR-27a mimic improves cardiac function and reduces atherosclerotic plaques development in *Apoe*$^{-/-}$ mice. (A) Representative M-mode echocardiography images (parasternal long-axis, PSLA view) of the left ventricle (LV) of control oligo or miR-27a-injected mice. (B) M-mode tracings were used to calculate LV parameters (viz. LV internal dimensions at diastole and systole, LVIDd, LVIDs; LV posterior wall thickness at diastole and systole, LVPWd and LVPWs) of control oligo (n=3) or miR-27a-treated mice (n=5). (C) Aortic arches were exposed and imaged under the microscope. The arrows indicate the plaques in the aortic arches and thoracic aorta. (D) High-resolution ultrasound images of the aortic arch of control oligo or miR-27a injected-mice. (E) Vessel wall thickness at the lesser curvature of the arch was calculated for control oligo or miR-27a group. (F) Representative images of liver sections from control oligo or miR-27a group stained with H & E and Oil Red O. Scale bar: 100 µm, total magnification X200. (G) Quantification of Oil Red O staining (% positive stained area) for lipid accumulation in the liver. (H) Representative photomicrographs of Picro Sirius

Red (PSR) stained liver sections under brightfield (PSR-BF) or polarized light (PSR-PL) to assess liver fibrosis are shown. Scale bar: 100 µm, total magnification X200. (I) Quantification of fibrosis area upon PSR staining is indicated. Statistical significance was determined by Student's *t*-test (unpaired, 2-tailed). * $p<0.05$ and ** $p<0.01$ as compared to the control oligo-injected group.

Fig.9. miR-27a regulates *Hmgcr* expression by translational repression. AML12 cells were transfected with 500 ng of miR-27a expression plasmid or pcDNA3.1 (as control). After 24 hrs of transfection, they were incubated with actinomycin D (5 µg/ml) for different time points. (A) Hmgcr mRNA levels were plotted relative to 0 hr time point as described in *SI Appendix, SI Materials and Methods* (B) Endogenous Hmgcr mRNA half-life estimation in AML12 cells on ectopic over-expression of miR-27a. The mRNA half-life of *Hmgcr* was measured over 24 hrs in the presence of 5 µg/ml of actinomycin D in control cells (transfected with pcDNA3.1) and miR-27a transfected AML12 cells. Hmgcr mRNA half-life is represented as mean ± SEM of three independent experiments. (C) Effect of transcriptional attenuation on endogenous Hmgcr protein levels in miR-27a over-expressed hepatocytes. AML12 cells transfected with either pcDNA 3.1 or miR-27a expression plasmid and incubated with actinomycin D for different time points. Western blot analysis of total proteins was carried out probing for Hmgcr and vinculin. The relative Hmgcr protein levels normalized to vinculin for different time points are also shown. The normalized Hmgcr levels as fold change over the control for every time point are also indicated. Statistical significance was determined by Student's *t*-test (unpaired, 2-tailed).

Fig.10. Augmentation of miR-27a represses cholesterol biosynthesis pathway. (A) Potential targets of miR-27a in the cholesterol biosynthesis pathway as predicted by *in silico* tools (viz. miRWalk, RNAhybrid and TargetScan) and categorized based on their molecular functions using PANTHER database. qPCR analysis for the predicted cholesterol biosynthesis genes was performed in (B) AML12 cells transfected with miR-27a mimic and (C) liver tissues of high cholesterol diet-fed *Apoe*$^{-/-}$ mice-injected with

miR-27a mimic or control oligo. Statistical significance was determined by Student's *t*-test (unpaired, 2-tailed). *p<0.05 and ** p<0.01 as compared to the control.

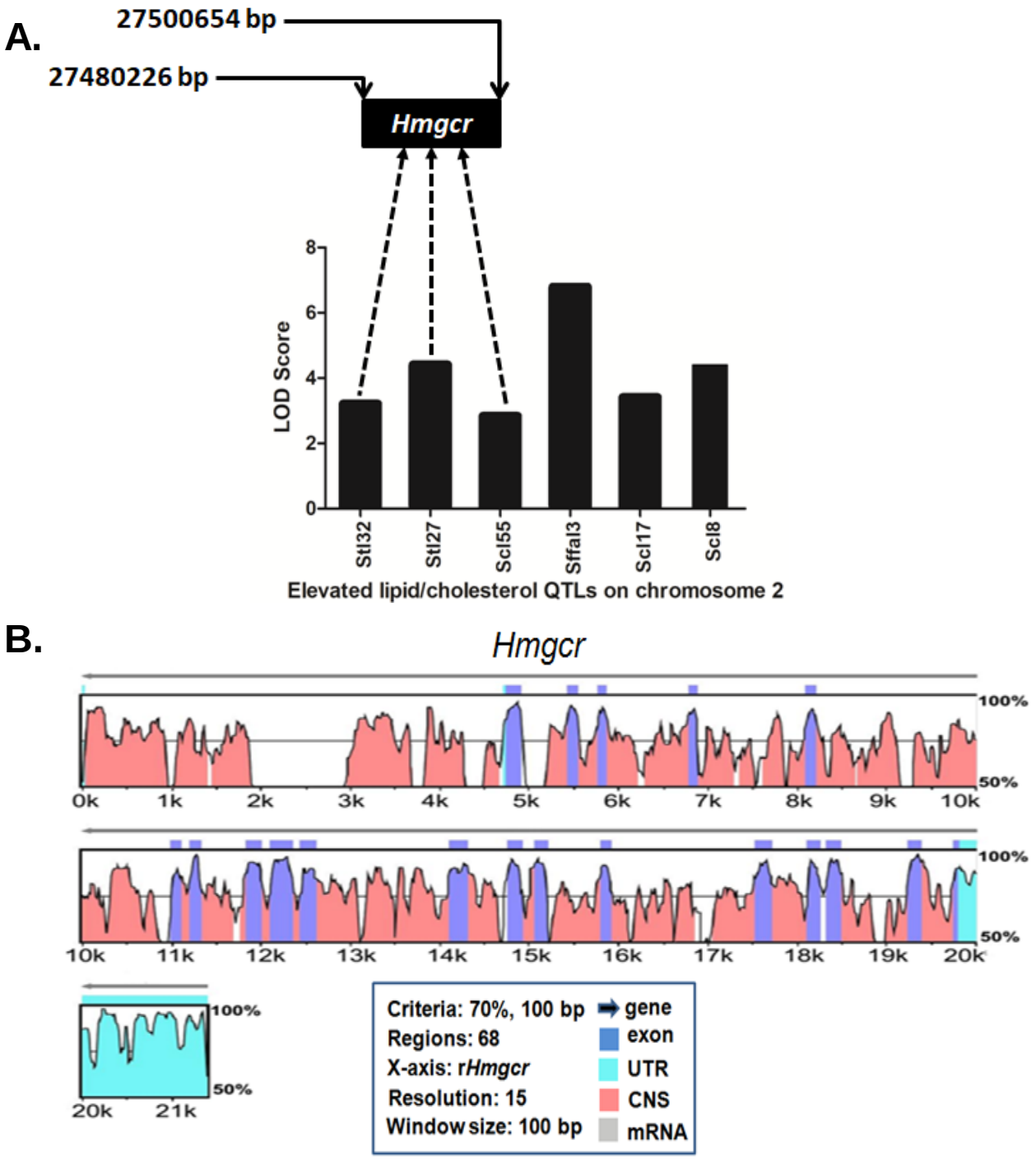

Figure 1

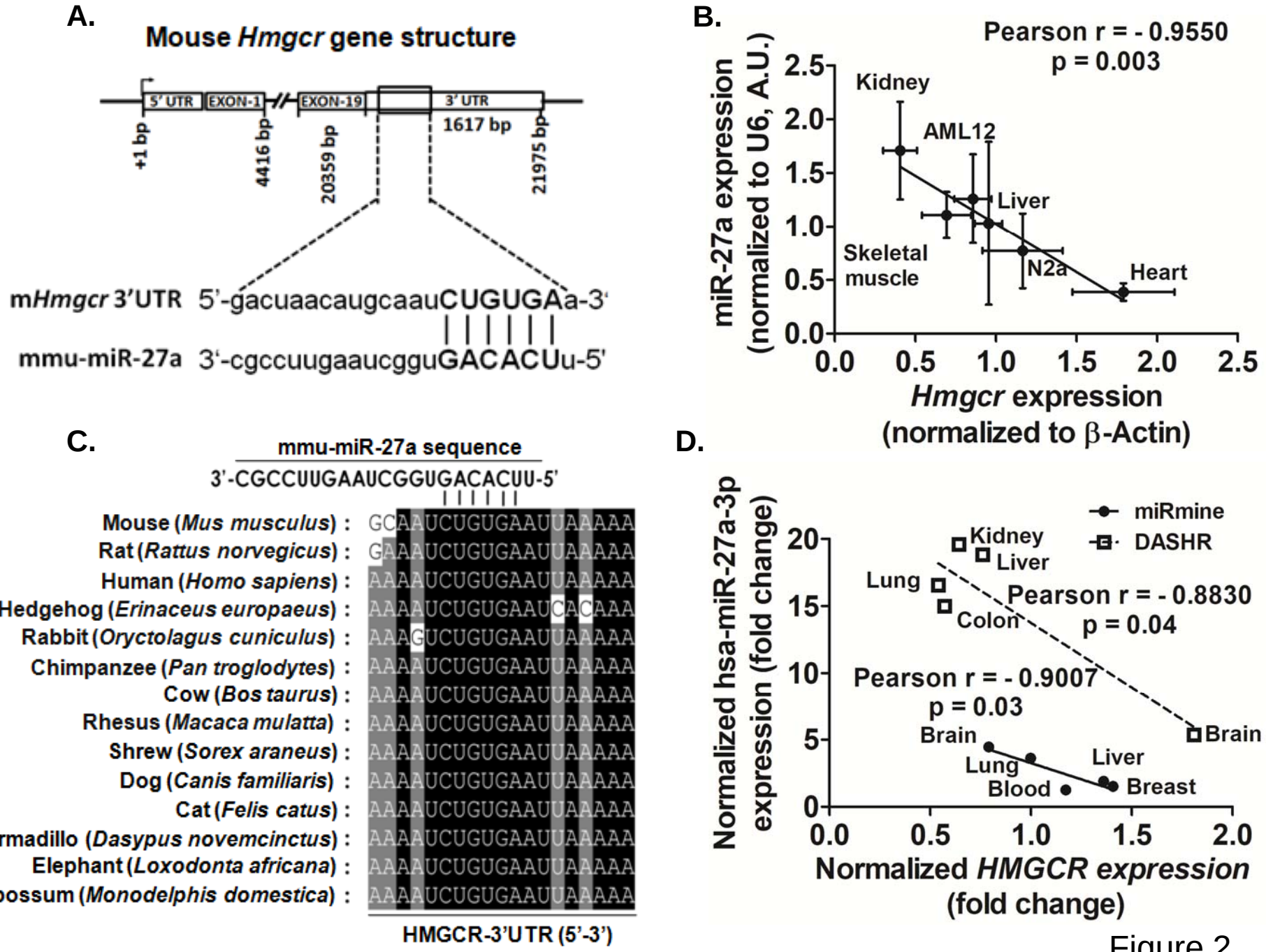

Figure 2

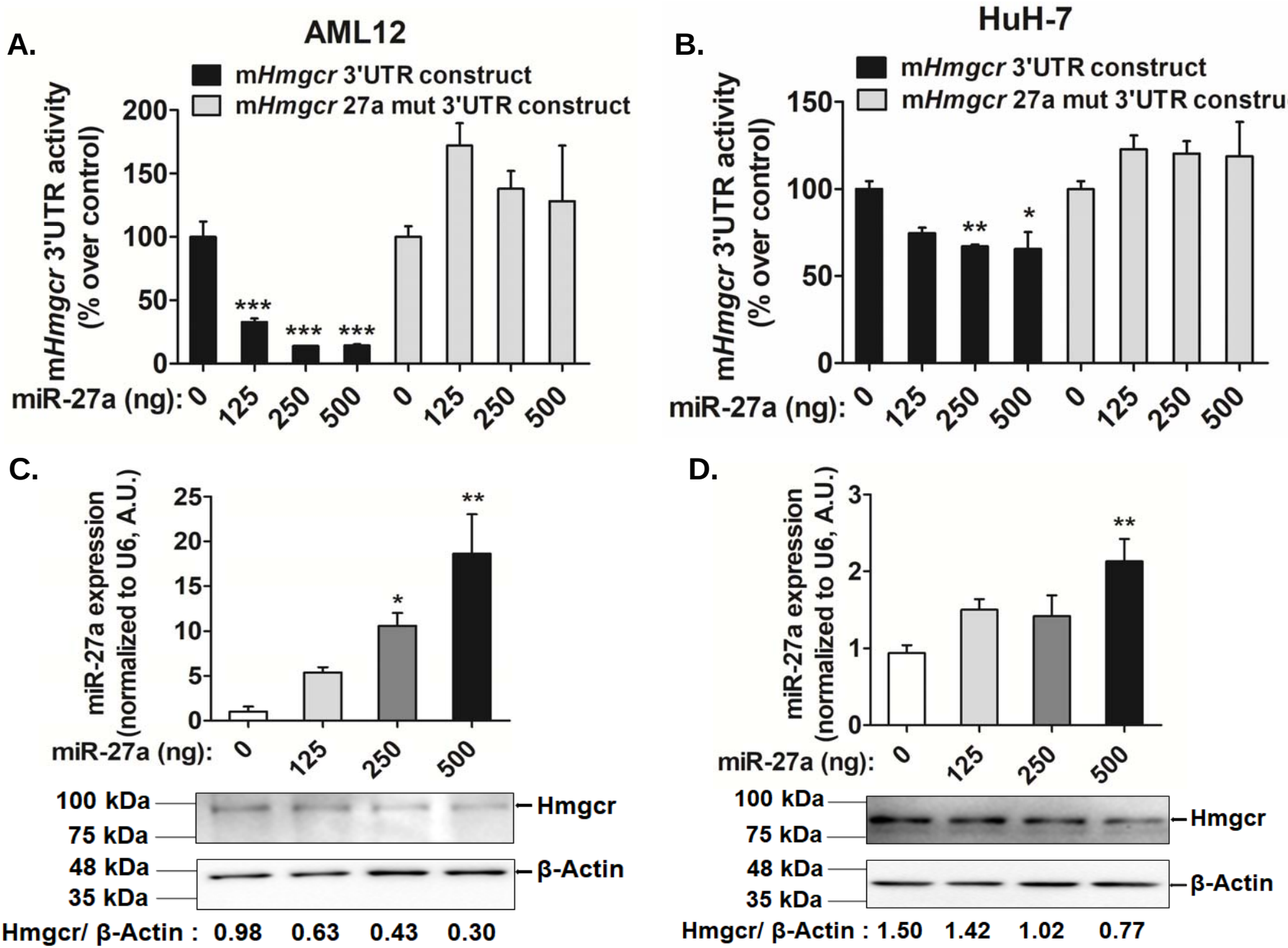

Figure 3

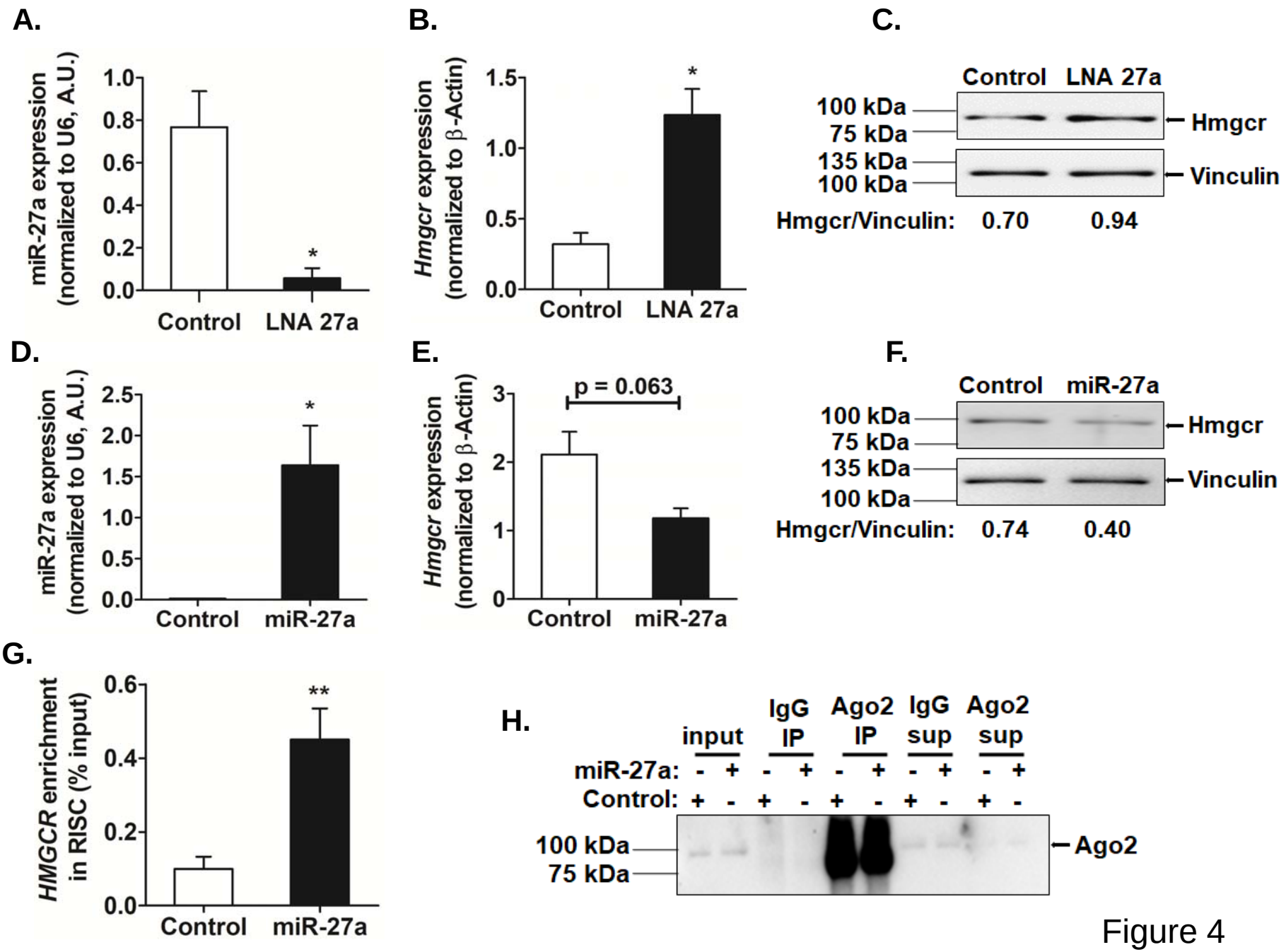

Figure 4

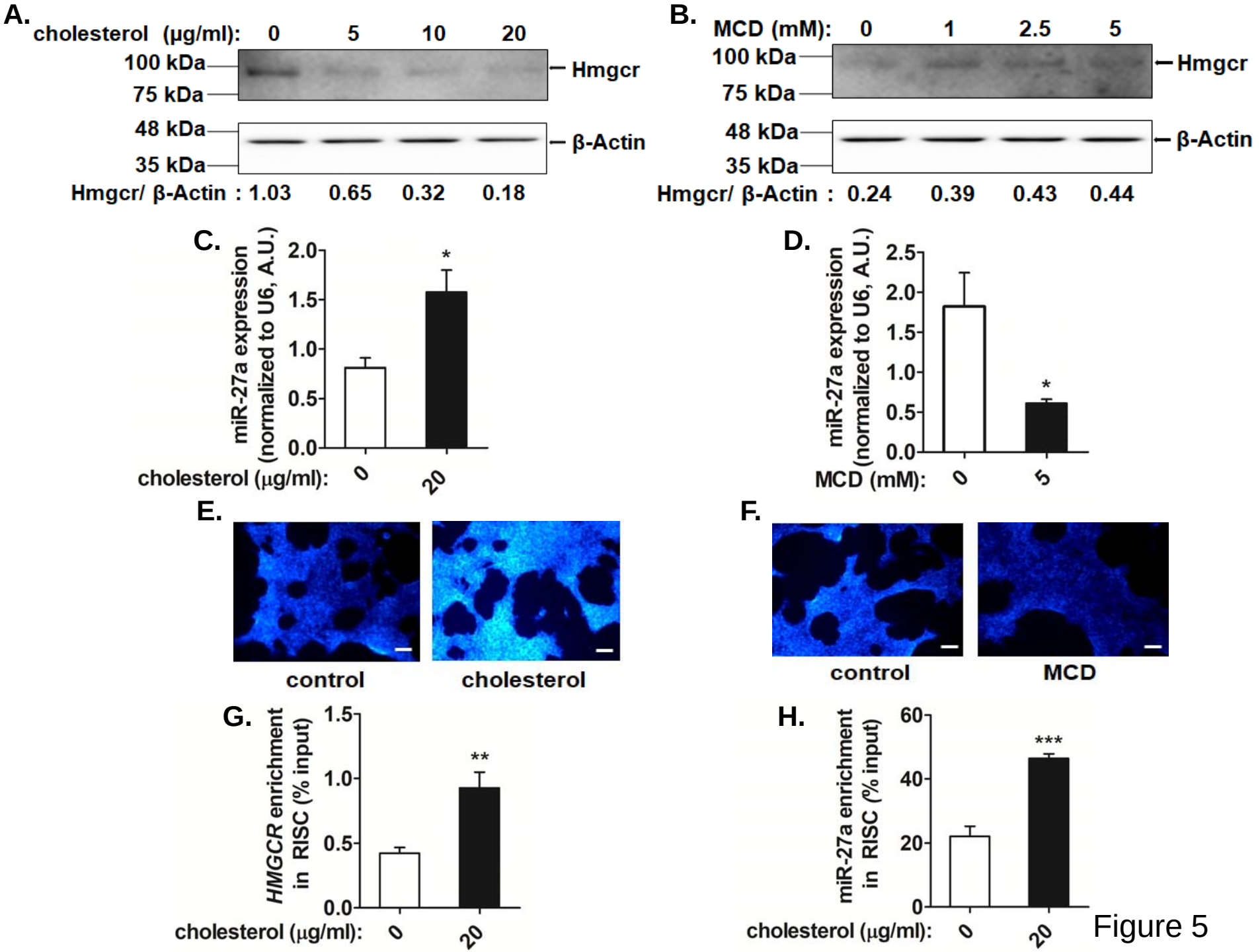

Figure 5

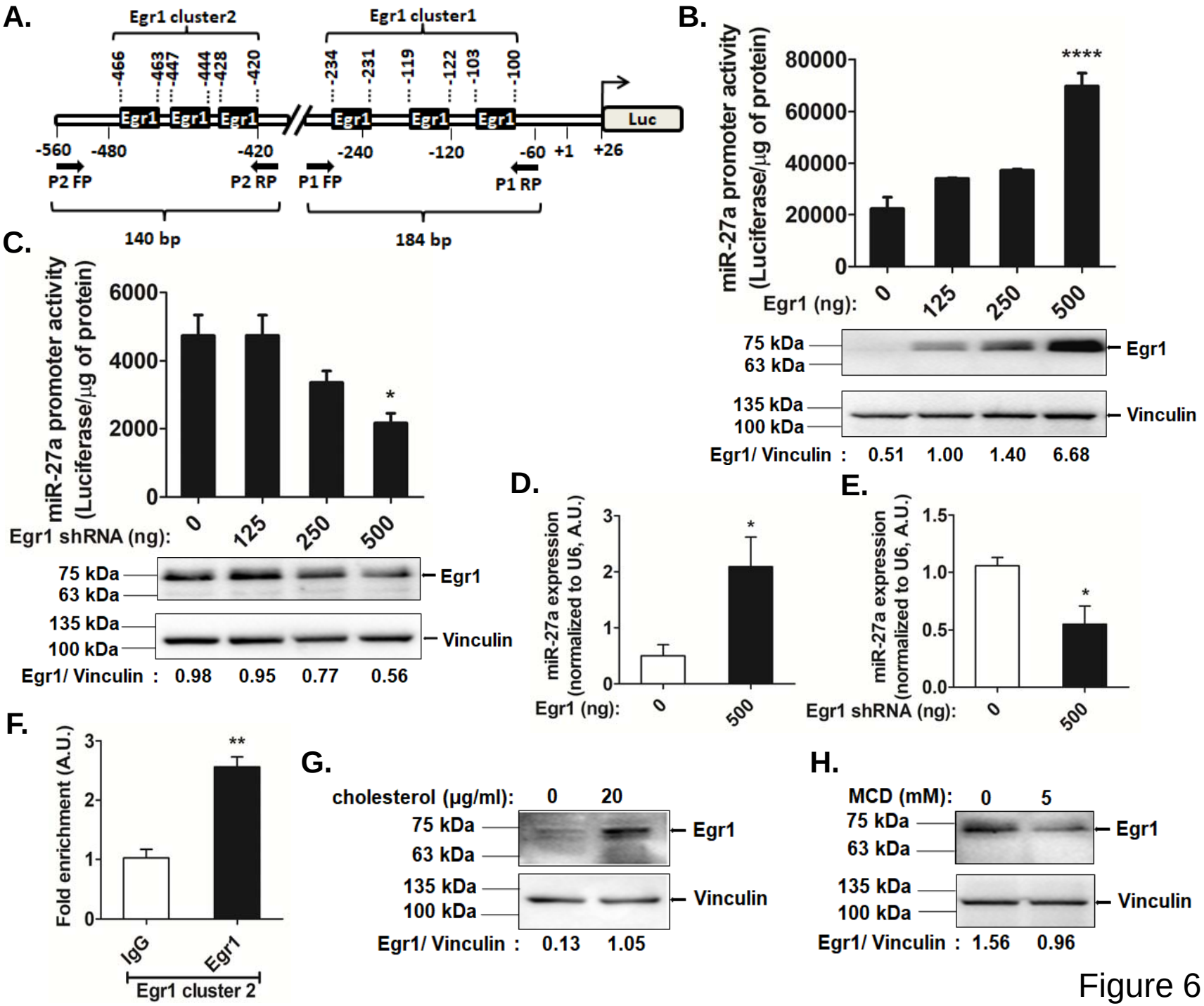

Figure 6

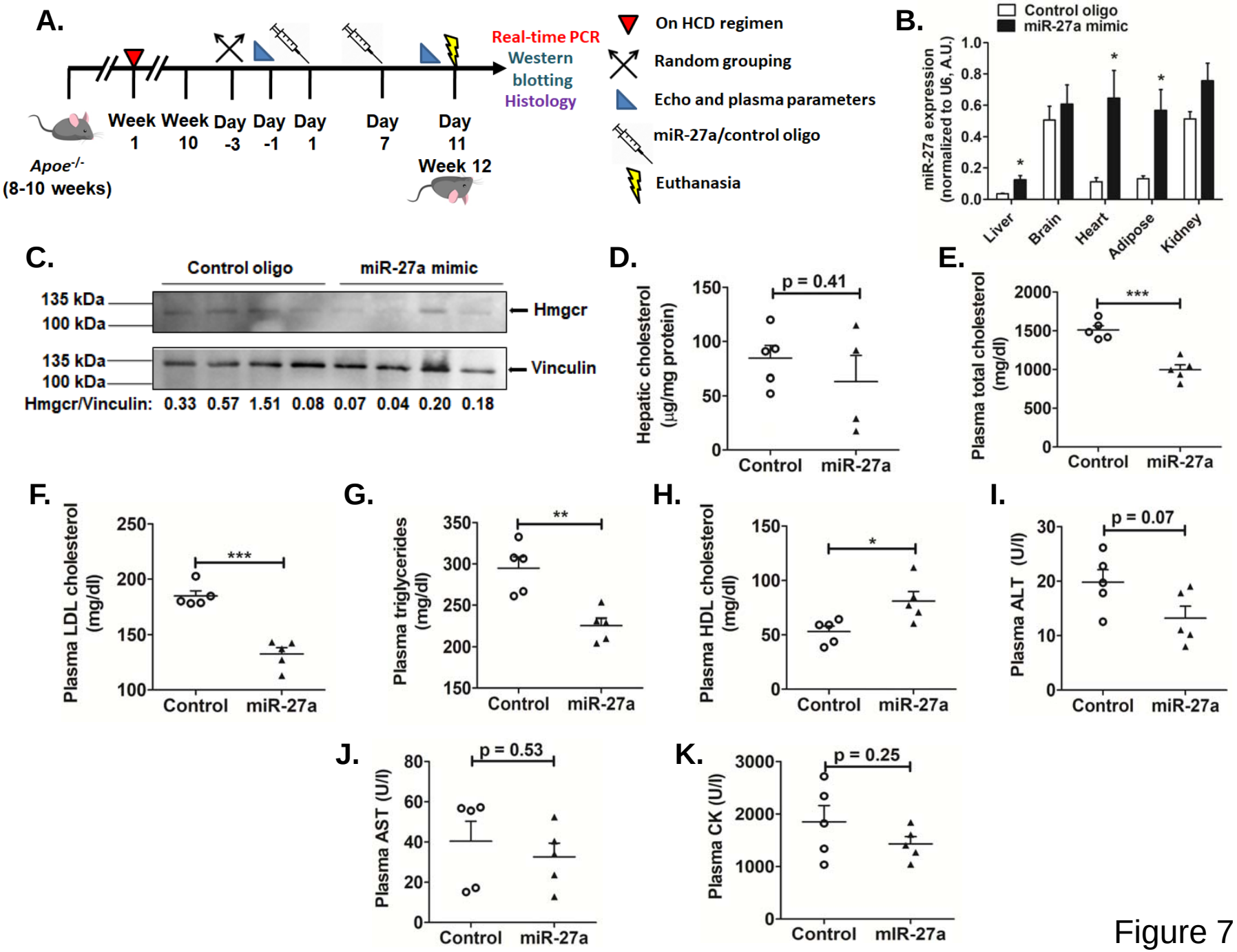

Figure 7

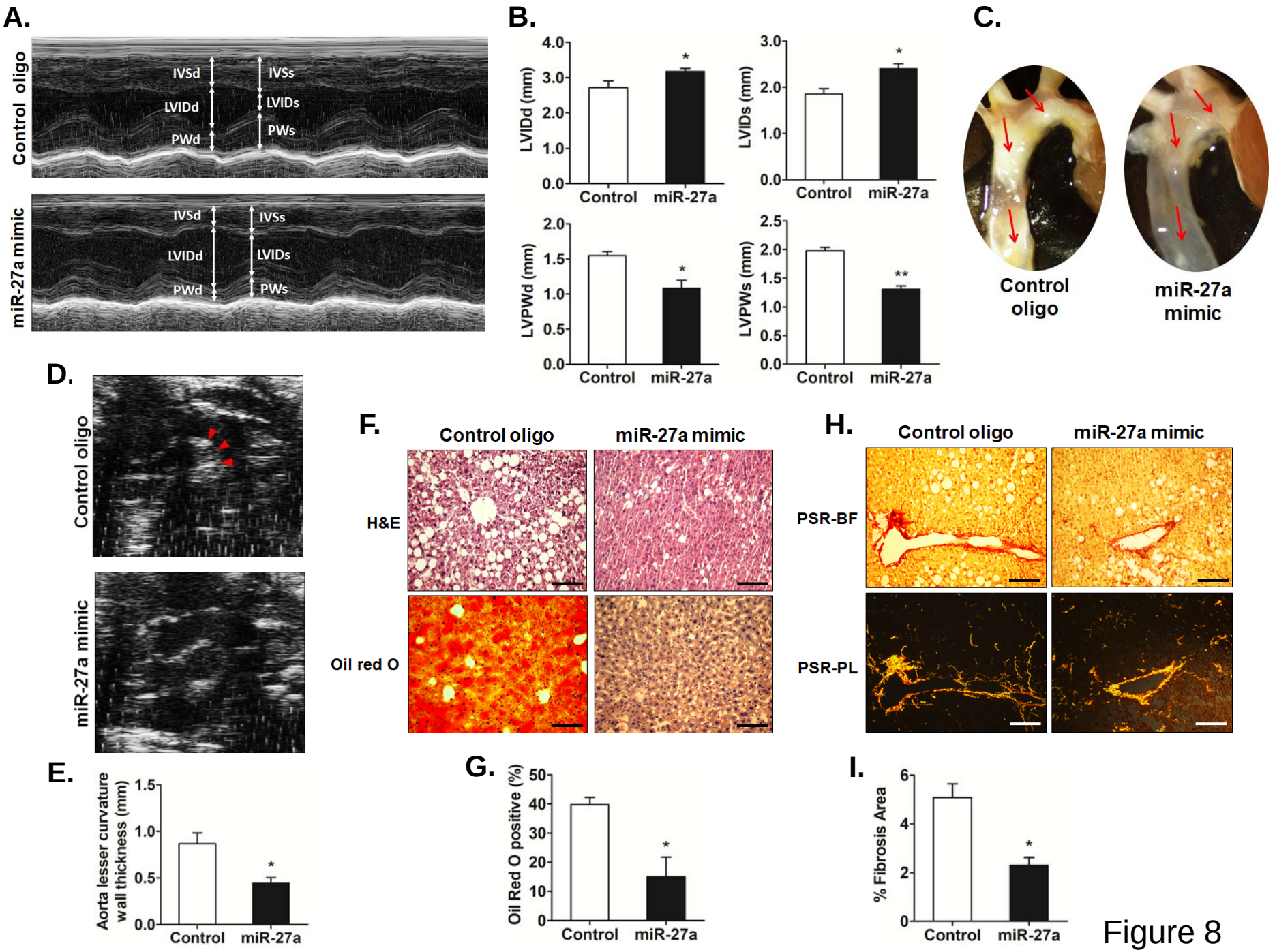

Figure 8

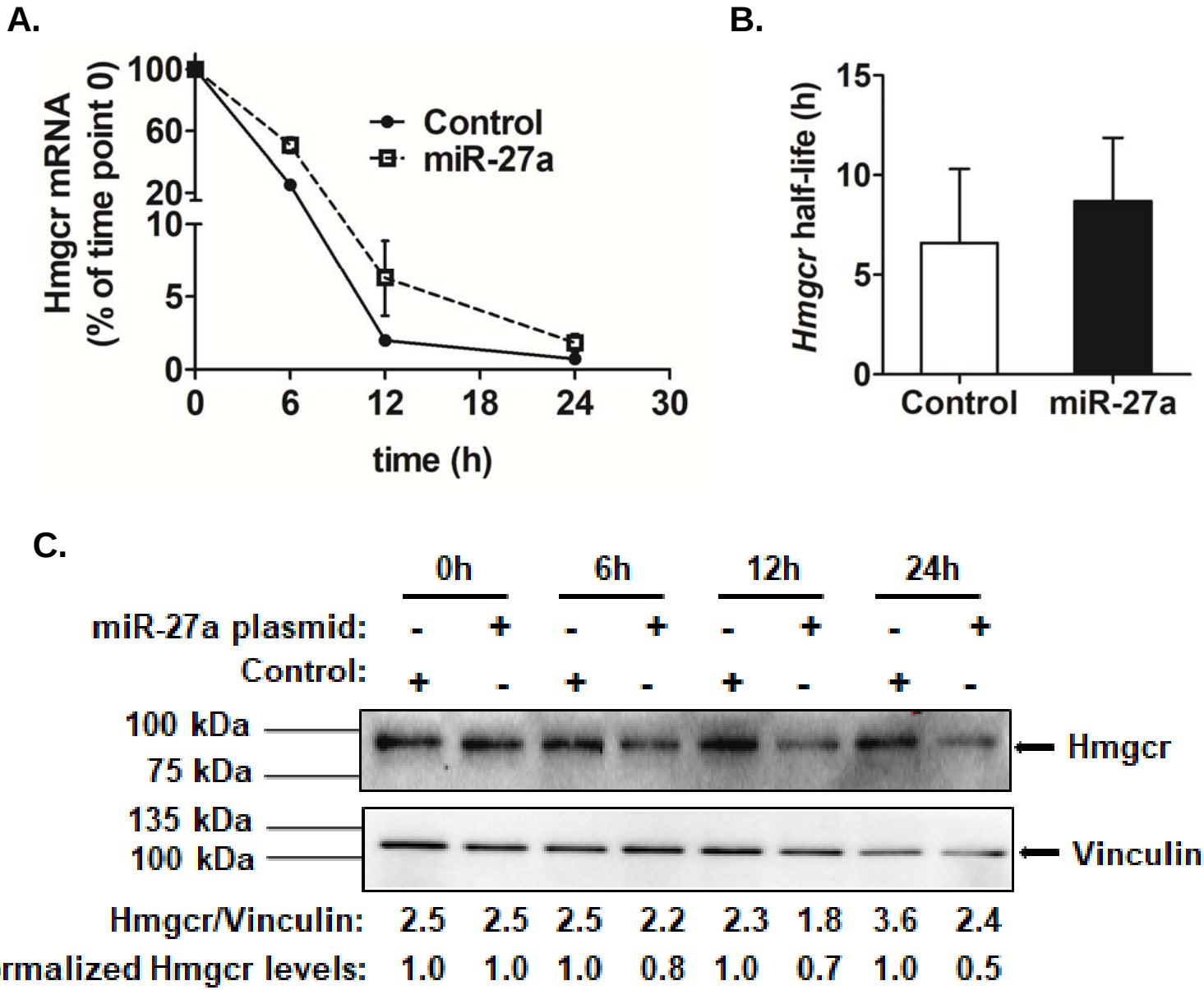

Figure 9

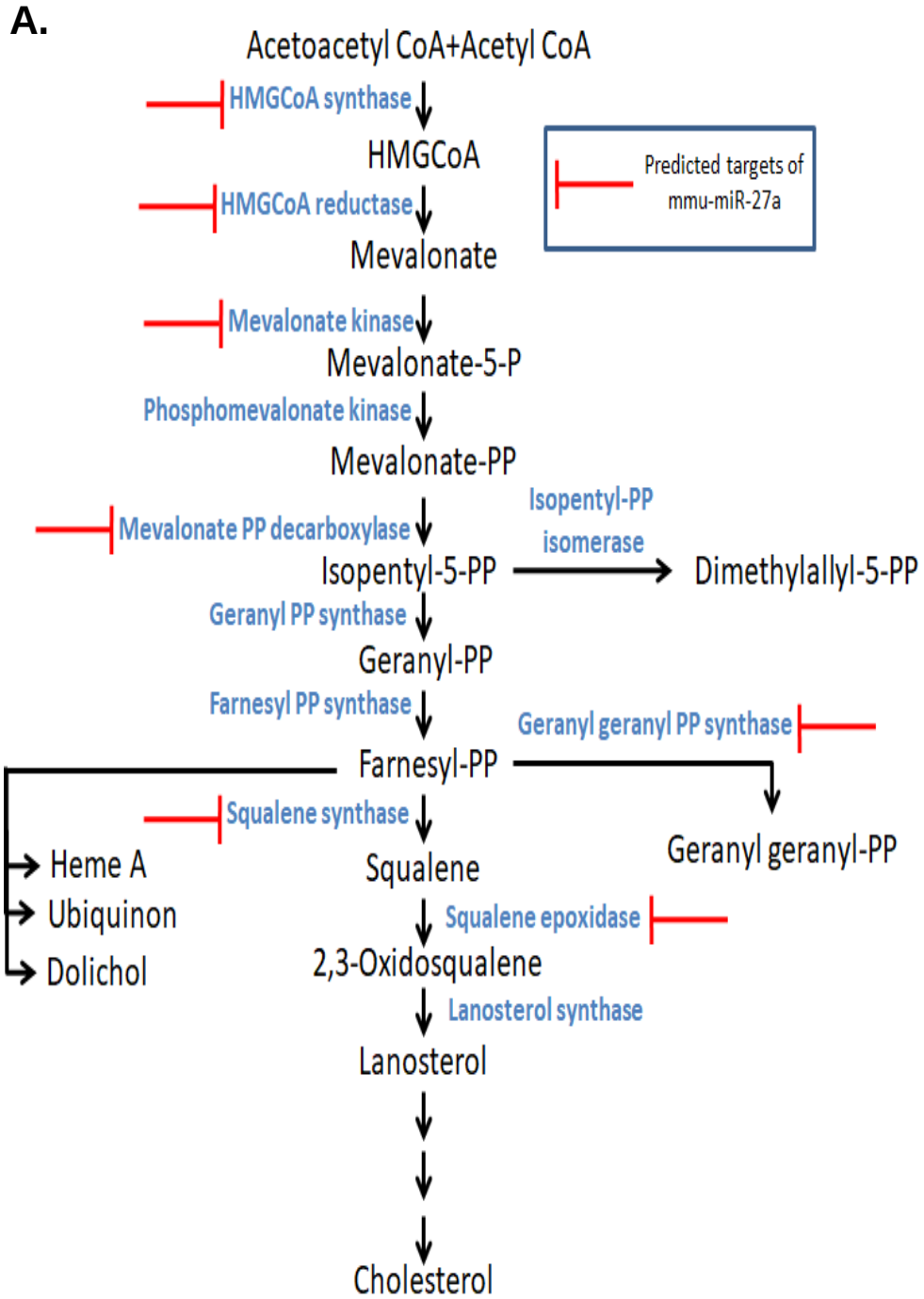

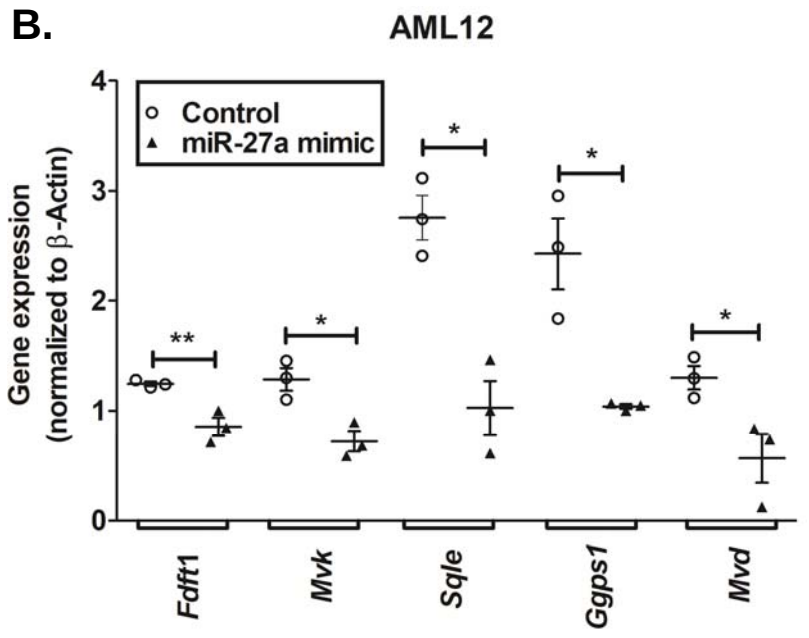

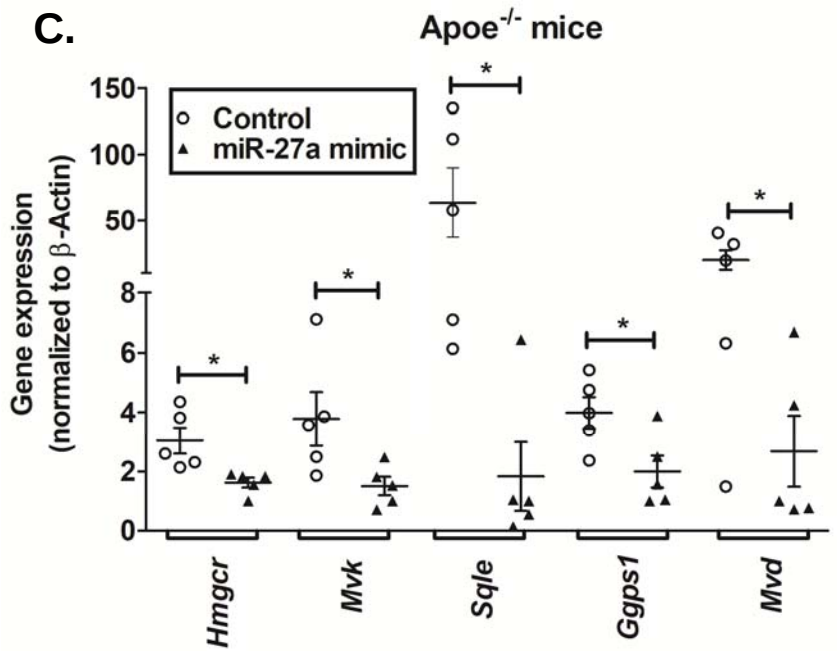

Figure 10